

1 **Evaluation of vegetation communities, water table, and peat composition as drivers of**
2 **greenhouse gas emissions in lowland tropical peatlands**

3
4
5
6 Jorge Hoyos-Santillan^{1*}; Barry H. Lomax¹; David Large²; Benjamin L. Turner³; Omar R.
7 Lopez⁴; Arnoud Boom⁵; Armando Sepulveda-Jauregui⁶; Sofie Sjögersten¹

8
9 ¹The University of Nottingham, School of Biosciences, Sutton Bonington Campus,

10 Loughborough LE12 5RD, UK

11 ²The University of Nottingham, Department of Chemical and Environmental Engineering,

12 Nottingham NG7 2RD, UK

13 ³Smithsonian Tropical Research Institute, Apartado 0843-03092, Balboa, Ancon, Republic of

14 Panama

15 ⁴Instituto de Investigaciones Científicas y Servicios de Alta Tecnología (INDICASAT)

16 Centro de Biodiversidad y Descubrimiento de Drogas Clayton Republic of Panama

17 ⁵University of Leicester, Department of Geography, Leicester LE1 7RH, UK

18 ⁶University of Magallanes, Department of Sciences and Natural Resources, Punta Arenas,

19 Chile

20 *Corresponding author:

21 Jorge Hoyos-Santillan

22 Email: jhoyosantillan@gmail.com

23 t: +56 973114861

24

25 **Abstract**

26

27 Tropical peatlands are globally important source of greenhouse gases to the atmosphere, but
28 data on carbon fluxes from these ecosystems is limited due to the logistical challenges of
29 measuring gas fluxes in these ecosystems. Proposals to overcome the difficulties of
30 measuring gas carbon fluxes in the tropics include remote sensing (top-down) approaches.
31 However, these require information on the effect of vegetation communities on carbon
32 dioxide (CO₂) and methane (CH₄) fluxes from the peat surface (bottom-up). Such information
33 will help reducing the uncertainty in current carbon budgets and resolve inconsistencies
34 between the top-down and bottom-up estimates of gas fluxes from tropical peatlands. We
35 investigated temporal and spatial variability of CO₂ and CH₄ fluxes from tropical peatlands
36 inhabited by two contrasting vegetation communities (*i.e.*, mixed forest and palm swamp) in
37 Panama. In addition, we explored the influence of peat chemistry and nutrient status (*i.e.*,
38 factorial nitrogen (N) and phosphorus (P) addition) on greenhouse gas fluxes from the peat
39 surface. We found that: i) CO₂ and CH₄ fluxes were not significantly different between the
40 two vegetation communities, but did vary temporally across an annual cycle; ii) precipitation
41 rates and peat temperature were poor predictors of CO₂ and CH₄ fluxes; iii) nitrogen addition
42 increased CH₄ fluxes at the mixed forests when the water table was above the peat surface,
43 but neither nitrogen nor phosphorus affected gas fluxes elsewhere; iv) gas fluxes varied
44 significantly with the water table level, with CO₂ flux being 80% greater at low water table,
45 and CH₄ fluxes being 81% higher with the water table above the surface. Taken together, our
46 data suggested that water table is the most important control of greenhouse gas emissions
47 from the peat surface in forested lowland tropical peatlands, and that neither the presence of
48 distinct vegetation communities nor the addition of nutrients outweigh such control.

49 **Keywords:** Camptosperma, methane, nitrogen, pyrolysis, phosphorus, Raphia

50 **1. Introduction**

51

52 Tropical peatlands represent an important component in the global carbon cycle (Dommain et
53 al., 2014; Sjögersten et al., 2014). They act simultaneously as carbon (C) sinks and sources;
54 holding belowground ≈ 119 Gt C (Leifeld and Menichetti, 2018), and emitting annually 1.23
55 Gt C-CO₂ and 0.068 Gt C-CH₄ (Sjögersten et al., 2014). Land use change (*e.g.*, drainage, land
56 clearing), and climate change (*e.g.* prolonged droughts) threaten C sequestration in tropical
57 peatlands by creating conditions that promote rapid decomposition of peat (Houghton, 2012;
58 Pearson et al., 2017; Turetsky et al., 2014). This can turn tropical peatlands into net carbon
59 emitters to the atmosphere (Couwenberg et al., 2010; Hoyos-Santillan et al., 2016a; Page et
60 al., 2011). Unfortunately, due to the logistical difficulties and demanding conditions that
61 prevail in these ecosystems, there are a limited number of studies that have recorded *in situ*
62 flux measurements. Consequently, the current estimates of greenhouse gas emission from
63 peatlands in tropical regions are highly uncertain (Kirschke et al., 2013; Lawson et al., 2015;
64 Tian et al., 2016). In order to reduce the uncertainties, further quantitative research on carbon
65 exchange in tropical peatlands has to be conducted (Couwenberg et al., 2010). In addition,
66 different approaches have been explored to develop proxies that, in conjunction with remote
67 sensing techniques, allow to evaluate greenhouse gas emission from large areas of tropical
68 peatlands without having to conduct massive field campaigns on a regular basis (Couwenberg
69 and Fritz, 2012).

70 Vegetation and water table have been previously suggested as proxies to estimate greenhouse
71 gas emissions from peatlands located in temperate regions (Couwenberg et al., 2011; Dias et
72 al., 2010); however, limited information exist with respect to their application in tropical
73 peatlands (Couwenberg et al., 2010). Vegetation exerts direct influence on greenhouse gas

74 emission through different mechanisms, for example: mediating gas transport to the
75 atmosphere through aerenchymatous structures and lenticels (Pangala et al., 2013, 2017);
76 allocating methanogens in woody tissue (Yip et al., 2018); modifying the redox conditions in
77 the rhizosphere by transferring oxygen into the peat matrix (Hoyos-Santillan et al., 2016a);
78 and releasing root exudates (Girkin et al., 2018). Vegetation also influences greenhouse gas
79 emission by controlling: water table level and peat hydraulic conductivity (Baird et al., 2017;
80 Couwenberg et al., 2011); the composition of litter and thus the peat forming material
81 (Hoyos-Santillan et al., 2015); the litter decomposition through the Home Field Advantage
82 effect (Hoyos-Santillan et al., 2018); and the functional structure of the microbial
83 communities (Troxler et al., 2012). Some of these factors vary on a diurnal (Hoyos-Santillan
84 et al., 2016a) and seasonal basis (Teh et al., 2017), further regulating greenhouse gas
85 emission in peatlands. Likewise, water table plays an important role in defining the
86 vegetation communities inhabiting a particular ecosystem. High water table limits the growth
87 of certain species but favors the development of others (Järveoja et al., 2016). In tropical
88 peatlands, in spite of fluctuations of the water table level, vegetation communities remain
89 stable in the short term. However, in the long term, water table participates in the formation
90 of domed structures (Phillips et al., 1997), in which the availability of nutrients varies from
91 the center of the dome towards the outer borders of the peat deposit, influencing the spatial
92 distribution of vegetation communities (*e.g.*, concentric arrangements) (Sjögersten et al.,
93 2011). Therefore, it is plausible that the spatial distribution of different vegetation
94 communities, and their associated characteristics, could be used as proxy to estimate the
95 magnitude of carbon emissions in these ecosystems.

96 Besides vegetation, nutrients availability also exert a direct influence on biogeochemical
97 processes in tropical peatlands (Hoyos-Santillan et al., 2018; Sjögersten et al., 2011). This
98 influence is particularly relevant in ecosystems subjected, directly or indirectly, to the

99 addition of fertilizers for agriculture practices (Oktarita et al., 2017). For example, the
100 addition of nitrogen has been observed to exert contrasting effects on greenhouse gas
101 emissions (*e.g.*, CO₂, nitrous oxide (N₂O)), increasing or decreasing their fluxes depending
102 on the type of nitrogen component applied (*e.g.* urea, nitrate, ammonium) (Khalil et al.,
103 2007), as well as the type of peat on which it is utilized (Comeau et al., 2016). In tropical
104 peatlands, nutrients are also related to the conformation and distribution of vegetation
105 communities in peat domes (Sjögersten et al., 2011). Thus, it is likely that the availability of
106 nutrients affects greenhouse gas emissions by shaping the spatial distribution of vegetation
107 species and simultaneously influencing heterotrophic respiration in the peat.

108 Neotropical peatlands are often forested by palms or evergreen broadleaved trees, forming
109 distinct vegetation communities (Draper et al., 2014; Sjögersten et al., 2011). For instance,
110 peat swamp forests in the Caribbean coast of Panama and Costa Rica typically support
111 monodominant stands of the canopy forming evergreen palm *Raphia taedigera* (Mart.)
112 (Hoyos-Santillan et al., 2016a; Myers, 1981; Phillips et al., 1997), or mixed forests composed
113 of palms and evergreen broadleaved hardwood trees (*e.g.*, *Camptosperma panamensis*
114 (Standl.)) (Phillips et al., 1997; Urquhart, 1999). These forests emit both CO₂ and CH₄ fluxes,
115 with seasonal and spatial variability in emissions related to both substrate availability (Girkin
116 et al., 2018b) and CH₄ oxidation processes (Wright et al., 2011, 2013).

117 In addition, CO₂ and CH₄ are produced in the subsurface layers of peat through the entire
118 stratigraphic profile (Hoyos-Santillan et al., 2016b; Wright et al., 2011). In domed peatlands,
119 the depth of the peat layer varies among peatlands with distinct vegetation communities. For
120 example, in Panama, the deepest peat deposits have been located at the top of the dome of the
121 Changuinola peatland (inhabited by mixed forest and sawgrass) and at the Damani-
122 Guariviara peatland (inhabited by mixed forest), reaching depths of 9.5 and 5.9 m,
123 respectively (Hoyos-Santillan et al., 2016b; Phillips et al., 1997).

124 To test the viability of using vegetation communities as proxy for greenhouse gas emission,
125 we monitored CO₂ and CH₄ surface emissions from two contrasting forest types, palm swamp
126 and mixed forest (Sjögersten et al., 2011). Three peatlands for each type of forest were
127 selected as study sites. The monitoring campaigns were distributed over one year, including a
128 dry and a wet season. This approach was used to test the following hypotheses: (i) different
129 vegetation communities present distinct magnitudes in their surface greenhouse gas fluxes;
130 (ii) greenhouse gas emissions vary throughout the year due to seasonal fluctuation of the
131 water table position; and iii) molecular composition of peat (*e.g.*, lignin, phenolic
132 compounds, and fatty acids content) influences greenhouse gas emissions from the peat's
133 surface. In addition, we conducted a N and P addition experiment in two sites, each one
134 covered with one of the two contrasting vegetation communities. This experiment tested the
135 hypothesis that (iv) addition of nutrients increases CO₂, CH₄, and N₂O emission in tropical
136 peatlands.

137

138 **2. Materials and methods**

139

140 **2.1 Site description**

141 The study was conducted in the north-west Caribbean coast of Panama where several large
142 peatlands are located within the Bocas del Toro province (Phillips et al., 1997). Rainfall
143 averages $3,092 \pm 181$ mm yr⁻¹, with a mean annual air temperature of 25.9 ± 0.3 °C (2003 to
144 2011; Smithsonian Tropical Research Institute Physical Monitoring Program). There is no
145 pronounced seasonality (Wright et al., 2011), although there are two periods of reduced
146 rainfall from February to April and August to September.

147 Seven phasic communities have been identified in these peatlands (Phillips et al., 1997). We
148 studied two of these: palm swamp dominated by *Raphia taedigera* (Mart.), a canopy forming
149 palm in the Arecaceae family, and mixed forest dominated by *Camposperma panamensis*
150 (Standl), an evergreen broadleaved hardwood tree in the Anacardiaceae family (Table 1; Fig.
151 S1). Three sites for each of these two types of vegetation communities were selected for this
152 study. The selection was based on their contrasting characteristics, considering that those
153 differences could potentially impact on greenhouse gas emissions from peat. For example, the
154 roots of *R. taedigera* palm are composed by hollow aerenchymatous tissue, including the
155 development of dense pneumatophores structures (Hoyos-Santillan et al., 2016a). These
156 structures are distributed throughout the upper peat layer, constituting a shallow (≈ 1.1 m
157 depth), but fibrous root system (Wright et al., 2011). This tissue participates in the reduction
158 of CH₄ emissions from peat, due to axial oxygen loss through *R. taedigera* root system
159 (Hoyos-Santillan et al., 2016a). By contrast, *C. panamensis* does not develop aerenchymatous
160 tissue but has woody lignified structural roots (≈ 1 m depth) with abundant surface knee roots
161 (Wright et al., 2011). This root system is not as dense as that of *R. taedigera* (Wright et al.,
162 2011), but does have lenticels to exchange gases with the atmosphere.

163 Palm sites had large amounts of palm leaf litter at the surface (Wright et al., 2011). The
164 mixed forest sites had large amounts of *C. panamensis* leaf litter at the surface but leaf litter
165 from other species was also present. Microtopography in these sites is characterized by an
166 uneven terrain, forming shallow ponds and raised areas (close to the trees associated with
167 root structures) (Hoyos-Santillan et al., 2016b). During the dry season, shallow ponds are no
168 longer present, due to the lowering of the water table, but the uneven microtopography
169 remains.

170 Peatlands selected for this study are freshwater ($< 200 \mu\text{S cm}^{-1}$) and their depth varies
171 between 1 to 6 m (Table 1). The water table in the peatlands fluctuates from + 0.15 to - 0.4 m

172 relative to the peat surface (Wright et al., 2011). The Changuinola peat deposit, where San
173 San Pond Sak 1 and 2 sites are located, is an 80 km² ombrotrophic domed peatland (Cohen et
174 al., 1989). The vegetation communities that formed the peat of the Changuinola peat deposit
175 and the Damani-Guariviara peatland have shifted over time, thus the peat composition varies
176 in botanical origin and its degree of humification through the stratigraphic profile (Hoyos-
177 Santillan et al., 2015; Phillips et al., 1997). The texture of the peat on the top layers of all
178 sites is coarse, mainly dominated by roots, whereas deeper layers have a finer composition
179 without recognizable litter, indicating a higher degree of decomposition (Hoyos-Santillan et
180 al., 2016b; Wright et al., 2011). In all the studied peatlands, the underlying mineral soil
181 reflected an estuarine-marine origin, formed by sand and macrofossils (*e.g.*, gastropod shells,
182 bivalves, and crustaceans) (Hoyos-Santillan, 2014).

183

184 2.2. Experimental programme and methodology

185

186 2.2.1 *Vegetation survey*

187 To characterise the two types of forest, vegetation inventories were conducted in 0.1 ha plots
188 (20 × 50 m); all stems > 0.1 m in diameter at breast height (DBH) were mapped, measured,
189 marked, and tagged. The basal area of the tree species found in the plots was calculated from
190 the DBH data. However, given the multi-stem colonial growth of *R. taedigera*, it is plausible
191 that basal area for this species was overestimated. The basal area for the San San Pond Sak
192 sites corresponds to those published by Sjögersten *et al.* (2011) (Table S1).

193

194 2.2.2 *Physicochemical parameters*

195 A sampling well was installed at each plot to measure the level of the water table, *in situ*
196 dissolved O₂, and temperature of the pore-water. These measurements were conducted at
197 each site on each sampling and monitoring event (Table S2). Each well consisted of a 50 mm
198 diameter PVC pipe with 10 mm diameter perforations at 50 mm intervals. The location of
199 each sampling well corresponds to those presented in Table 1. Dissolved O₂ (DO; mg L⁻¹)
200 and temperature (°C) were measured at the top 0.5 m of the peat profile at the sampling wells
201 using a portable multiparametric probe (YSI 556 MPS, USA). Water table level was
202 measured with a measuring tape at the sampling well of each site, in relation to the peat's
203 surface. In addition, in order to account for the heterogeneity of the microtopography, water
204 table position was assigned a categorical classification. The classification considered the
205 position of the water table with respect to the peat's surface in the sites were the static
206 chambers for measuring gases, were installed. The criteria used to assign the categories was:
207 below peat surface (< 5 cm), at the surface (± 5 cm) or above the peat surface (> 5 cm). In
208 the case of shallow ponds, the above the surface category was applied. Three samples of peat
209 from the top 0.1 m layer of each site were used to conduct the physicochemical
210 characterization. Peat pH and conductivity were determined in a 1:2.5 peat fresh weight (fw)-
211 deionized water solution. Total C, nitrogen (N), and sulphur (S) were measured from 0.5 g
212 homogenised peat samples by using a total element analyser (Thermo Flash EA 1112, CE
213 Instruments, Wigan, UK). Peat ash was dissolved in 6 M HNO₃ to estimate the peat
214 phosphorus (P) concentration by molybdate colorimetry (Andersen, 1976). For detailed
215 methods see Hoyos-Santillan (2014).

216

217 *2.2.3 Monitoring temporal variations on greenhouse gas fluxes*

218 We measured greenhouse gas fluxes at three palm swamp forests dominated by *R. taedigera*
219 and three mixed forest dominated by *Camposperma panamensis* (Table 1, Fig. S1). Fluxes
220 were measured on six occasions at each plot; three occasions during dry and three during wet
221 season, respectively (December 2010 – September 2011, specific sampling dates are
222 presented in Table S2). During each monitoring event, we measured greenhouse gas fluxes at
223 three randomly chosen locations by triplicate within each plot. However, if shallow ponds
224 were present within the plot due to microtopography and hydrology heterogeneity, three
225 locations were selected to measure on top of the shallow ponds and three were selected in
226 non-flooded areas. Thus, up to eighteen chambers were installed for the collection of gases at
227 each plot during a single monitoring event. All fluxes were measured during daylight,
228 between 10:00 and 16:00 h.

229 We used the static chamber technique to measure the greenhouse gas fluxes (Sjögersten et al.,
230 2011). The chambers were made of opaque material, covering a 0.075 m² area, with a 0.1 m
231 height, and 7 L volume. Each chamber had a sampling port equipped with a Suba-Seal[®]
232 rubber septa. Although the forest floor was mostly unvegetated, trailing understory vegetation
233 and fallen branches were removed, before the installation of the chamber. Peat disturbance
234 was avoided as much as possible during the installation of the chambers, but slight pressure
235 was applied to ensure an air-tight seal. Chambers were left to stabilize for approximately
236 thirty minutes. This time period was used to install all chambers within the site and measure
237 physicochemical parameters at the sampling well. Once installed and stabilized, prior to the
238 collection of gas samples, the chamber headspace was homogenised by repeatedly pumping
239 the air within the chamber with a 20 mL syringe equipped with a hypodermic needle.
240 Afterwards, gas samples were collected from each chamber after 0, 2, 10 and 20 min and
241 stored in Exetainers (Labco, Lampeter, UK). All samples were shipped to the University of
242 Nottingham (Nottingham, UK) for analysis via gas chromatography. Vials were discarded for

243 chromatographic analyses if overpressure was absent (< 5 %). CO₂ and CH₄ concentrations
244 were determined using a single injection system with a 1 mL sample loop that passed the gas
245 sample using N₂ as carrier through a non-polar methyl silicone capillary column (CBP1-
246 W12-100, 0.53 mm I.D., 12 m, 5 mm; Shimadzu UK LTD, Milton Keynes, UK) and porous
247 polymer packed column (HayeSep Q 80/100). Thermal conductivity (TCD), flame ionization
248 (FID) and electron capture detector (ECD) were used to measure CO₂, CH₄, and N₂O,
249 respectively. Flux calculations were based on the linear accumulation of gases within the
250 closed chamber; gas samples that did not follow a linear accumulation trend were discarded
251 for the calculation of gas fluxes. The fluxes presented in this study do not separate
252 heterotrophic (mainly from peat and labile organic matter) from autotrophic (mostly derived
253 from roots) respiration (Lawson et al., 2015), and do not consider the greenhouse gas
254 transport mediated through vegetation.

255

256 *2.2.4 Nutrient addition experiment*

257 The potential role of nutrient limitation on greenhouse gas emission was explored by a
258 fertilization experiment. The experiment was conducted on two of the six sites selected for
259 this study; specifically, at San San Pond Sak 1 (palm swamp) and San San Pond Sak 2 (mixed
260 forest) in the Changuinola peat deposit (Table 1, Fig. S1). These sites were selected due to
261 the existing information from this peatland in relation to nutrient availability across distinct
262 vegetation communities (Sjögersten et al., 2011). The nutrient treatments were: N, P, N+P,
263 and control (Ctrl). The experiment consisted of ten blocks distributed along 150 m transects
264 running from south-east to north-west at the palm swamp and the mixed forest site (20 blocks
265 in total) (Fig. S1). Each block was 10 × 10 m with the nutrient enrichment treatments applied
266 at each corner, blocks were 5 m apart. Adjacent corners had the same nutrient treatment. Thus

267 all twenty blocks (10 per vegetation community) had Ctrl, N, P, and N+P treatments (Fig.
268 S2). For further details on the experimental set up please refer to Hoyos-Santillan et al.,
269 (2018).

270 Nutrient enrichment was applied at the beginning of the experiment (October 2011) by filling
271 25 cm sections of dialysis tubing (Spectra/Por[®] membrane: 40mm diameter, 6000 to 8000
272 molecular weight cut off) with 0.86 mol of either N (Urea: CO(NH₂)₂) or P (calcium
273 phosphate monobasic monohydrate: Ca(H₂PO₄)₂•H₂O) fertilizer. This allowed a slow release
274 of nutrients through the membrane (Feller, 1995). After five months (March 2012), soil
275 samples were collected to evaluate the impact of the nutrient treatments on surface peat
276 properties (*i.e.* extractable and microbial nutrients) (Table S3). To do this, 10 × 10 × 10 cm
277 samples of peat were carefully cut from the surface peat. Soil samples were stored in plastic
278 bags at 4 °C for one week prior to nutrient analyses. Dissolved organic C (DOC) and
279 dissolved N fractions (TDN = dissolved organic nitrogen (DON) + inorganic fraction (nitrate-
280 nitrite and ammonium)) were extracted from surface peat (10 cm depth) and determined after
281 a five-fold dilution with a TOC-TN analyser (Shimadzu, Columbia, MD) (Sjögersten et al.,
282 2011). Readily-exchangeable P was extracted with anion exchange membranes (AEM)
283 (Myers, Thien & Pierzynski 1999; Turner and Romero 2009) and determined by automated
284 molybdate colorimetry using a flow injection analyser (Lachat Quikchem 8500, Hach Ltd,
285 Loveland, CO). To estimate if the nutrient treatment affected microbial activity in the peat,
286 extractable and microbial biomass C, N, and P were determined. Microbial C and N were
287 estimated by CHCl₃ fumigation (Brookes et al., 1982; Vance et al., 1987), whereas microbial
288 P was estimated by hexanol fumigation by resin strips (Myers et al., 1999; Turner and
289 Romero, 2009). For further details see Hoyos-Santillan *et al.* (2018). For this experiment,
290 surface greenhouse gas fluxes were measured before (October 2011) and five months after
291 the addition of the nutrients (March 2012). Measurements were conducted at each of the

292 twenty blocks on each treatment location (4 treatments × 10 blocks × 2 vegetation
293 communities).

294

295 2.2.5 Thermochemolysis

296 Tetramethylammonium-pyrolysis-gas chromatography-mass spectrometry (TMAH-Py-
297 GC/MS) was used to characterize the organic composition of peat. Treating the peat samples
298 with tetramethylammonium prior to Py-GC/MS analysis (i.e. TMAH-Py-GC/MS or
299 thermochemolysis) prevents thermal degradation of lignin-derived monomers (monolignols)
300 found in peat, as well as large fatty acids derived from plants epicuticular waxes or
301 microorganisms (Steward et al., 2009). Individual compound concentrations were estimated
302 by integrating the areas obtained in the pyrogram and calculating its corresponding
303 concentration using the 5- α -cholestane as an internal standard; concentrations were expressed
304 in relation to the total C content in the peat sample as $\mu\text{g compound mgC}^{-1}$. TMAH-Py-
305 GC/MS products were assigned a chemical class based on their molecular similarity to its
306 probable source molecule (Hoyos-Santillan et al., 2015; Schellekens, 2013). For this study,
307 lignin, fatty acids and phenolic compounds were grouped. The short and long chain
308 methylated fatty acids (Short < C20 and Long > C20) were further grouped into separate
309 categories to be used as independent covariates. Data corresponding to the TMAH-Py-
310 GC/MS analyses as well as further details on the methodology can be consulted in Hoyos-
311 Santillan *et al.* 2016b.

312

313 2.3 Statistical analyses

314

315 Linear mixed models were used to analyse gas fluxes and were fitted by using Residual
316 Maximum Likelihood (REML). Gas fluxes were transformed (\log_{10}) to fulfil the homogeneity
317 of variance requirements of the linear models. Level of significance of the differences
318 between the fixed effects was estimated by Wald tests using an F distribution ($P < 0.05$). For
319 the analysis of the seasonal variation of greenhouse gas fluxes, the vegetation community,
320 water table level, and season were used as fixed factors, while the specific site was included
321 as random factor. Water table level for the analysis was categorized as: below peat surface (<
322 5 cm), at the surface (± 5 cm) or above the peat surface (> 5 cm). The fluxes included in these
323 analyses comprise the six monitoring events at each site. For the analysis of variation of
324 greenhouse gas fluxes in relation to nutrient addition, the vegetation community and
325 treatment was used as a fixed factor, whereas the block was included as random factor.
326 Relationships between gas fluxes (\log_{10} transformed) and physicochemical characteristics of
327 surface peat (top 50 cm of peat layer) (*e.g.*, peat depth, rainfall, dissolved O₂, lignin, fatty
328 acids (short and long), phenolic compounds) were explored using regression analyses. The %
329 of variance accounted (adjusted R²) is presented in the figures. Results through text and
330 tables are presented as mean \pm SE. All statistical analyses were performed using GenStat
331 (14th edition, VSN International, 2011).

332

333 3. Results

334 3.1 Vegetation survey and nutrients

335 Vegetation survey data indicated that at the Chiriqui, Cricamola and San San Pond Sak 1
336 sites, *R. taedigera* was the dominant species; whereas at the San San Pond Sak 2, Almirante
337 and Damani-Guariviara sites, *C. panamensis* dominates (Table 1; Table S1). The deepest core
338 was collected at the Damani-Guariviara site, followed by the San San Pond Sak 2 site, both
339 dominated by *C. panamensis*; whilst the shallowest core was recorded at the Chiriqui site
340 dominated by *R. taedigera*. The total depth of the peat deposit was independent of the
341 vegetation community that currently dominates the area ($F_{1,4} = 0.94$, $P > 0.05$). Similarly,
342 total nutrients at the top layer of peat did not varied significantly with respect to the
343 vegetation community (TC: $F_{1,4} = 0.05$, $P > 0.05$; TN: $F_{1,4} = 0.2$, $P > 0.05$; TS: $F_{1,4} = 3.2$, $P >$
344 0.05 ; TP: $F_{1,4} = 3.4$, $P > 0.05$) (Table 2).

345

346 3.2.1 Spatial and temporal variation of greenhouse gas fluxes

347 No significant difference of the CO₂ and CH₄ fluxes between the two vegetation communities
348 was observed, *i.e.*, palm swamp and mixed forest (Fig. 1; Table 3). However, the water table
349 position with respect to the peat surface did influence both CO₂ and CH₄ emission (Fig. 2 and
350 3; Table 3).

351 In palm swamps, CH₄ fluxes presented a mean value of $3.99 \pm 0.6 \text{ mg m}^{-2} \text{ h}^{-1}$, with higher
352 values being observed when the water table was located above the peat surface ($> 5 \text{ cm}$; 6.33
353 $\pm 1.30 \text{ mg m}^{-2} \text{ h}^{-1}$) in comparison with the water table being located below the surface (< 5
354 cm ; $3.5 \pm 0.64 \text{ mg m}^{-2} \text{ h}^{-1}$). For mixed forest, the mean CH₄ flux was $3.19 \pm 0.59 \text{ mg m}^{-2} \text{ h}^{-1}$.
355 Parallel to palm swamp, higher CH₄ flux from mixed forest occurred when the water table

356 was above the peat surface ($4.25 \pm 1.07 \text{ mg m}^{-2} \text{ h}^{-1}$), in comparison with the $3.05 \pm 1.2 \text{ mg m}^{-2}$
357 h^{-1} observed when the water table was below the peat surface. The highest CH_4 flux
358 registered for mixed forest and palm swamp were $48.89 \text{ mg m}^{-2} \text{ h}^{-1}$ (water table: - 5 cm) and
359 $38.78 \text{ mg m}^{-2} \text{ h}^{-1}$ (water table: 8 cm), respectively. In the case of CO_2 , higher fluxes were
360 observed when water table was located below the peat surface for both palm swamp ($383 \pm$
361 $25 \text{ mg m}^{-2} \text{ h}^{-1}$) and mixed forest ($376 \pm 25 \text{ mg m}^{-2} \text{ h}^{-1}$) (Fig. 3). The highest CO_2 flux for
362 mixed forest and palm swamp were $913.18 \text{ mg m}^{-2} \text{ h}^{-1}$ (water table: - 30 cm) and 719.94 mg
363 $\text{m}^{-2} \text{ h}^{-1}$ (water table: - 20 cm), respectively. Both CO_2 and CH_4 fluxes varied significantly
364 through the year (Fig. 1, Table 3). The CO_2 flux followed a seasonal pattern, increasing
365 during periods of low rainfall and water table draw down (Fig. 1a,b). By contrast, the CH_4
366 flux did not follow a seasonal trend associated to precipitation (Fig. 1c,d).

367

368 3.2.2 Greenhouse gas flux and peat physicochemical characteristics

369 Among the physicochemical variables that were explored by linear regression (*e.g.*, water
370 table level, C:N ratio, methylated fatty acids, lignin content), only water table had a
371 significant inverse linear relationship with CO_2 flux (Fig. 4; Table S4). However, it is
372 important to consider that, the amount of variance accounted by the model predicting CO_2
373 flux from water table levels was low (*i.e.*, $R^2 = 0.15$). Long chain fatty acids ($> \text{C}_{20}$), which
374 represent a relatively labile substrate in peat, had a significant inverse linear relationship with
375 CH_4 flux ($R^2 = 0.15$; Table S4). A qualitative difference between the composition of surface
376 peat chemistry between the two phasic communities (*i.e.*, mixed forest and palm swamp) has
377 been previously reported (Hoyos-Santillan et al., 2016b). This difference is mainly related to
378 the relative abundance of distinct lignin moieties (*e.g.*, *p*-coumaryl, coniferyl, and sinapyl),
379 which are related to the recalcitrance of organic matter. However, although lignin and

380 phenolic compounds abundance is related to organic matter quality, they did not present a
381 significant linear regression model for CO₂ or CH₄ (Table S4).

382

383 3.3 Effect of nutrient addition on greenhouse gas fluxes

384 Five months after the addition of nutrients *in situ* at the San San Pond Sak peatland (San San
385 Pond Sak 1 – palm swamp and San San Pond Sak 2 - mixed forest; Fig. S1), N and P did not
386 affect the content of dissolved organic carbon at the top peat layer of the study sites (DOC-
387 N_{addition}: $F_{1,29} = 1.53$, $P > 0.05$; DOC-P_{addition}: $F_{1,29} = 0.02$, $P > 0.05$) (Hoyos-Santillan et al.,
388 2018). However, the addition of nitrogen did significantly increase the content of total
389 dissolved nitrogen in the surface peat (TDN-N_{addition}: $F_{1,28} = 8.71$, $P < 0.01$) and the addition
390 of P increased the content of readily-exchangeable P in the upper layer of peat (REP-P_{addition}:
391 $F_{1,56} = 7.67$, $P < 0.01$) (Table S5) (Hoyos-Santillan et al., 2018).

392 During the greenhouse gas monitoring event at the fertilized sites, water table was 10 cm
393 above the peat surface at the mixed forest and 25 cm below the peat surface at the palm
394 swamp. Fluxes of CO₂, CH₄, and N₂O were significantly different between the two vegetation
395 communities (CO₂-Vegetation community: $F_{1,18} = 12.79$, $P < 0.01$; CH₄-Vegetation
396 community: $F_{1,14} = 53.82$, $P < 0.001$); N₂O-Vegetation community: $F_{1,13} = 138$, $P < 0.001$).
397 Nutrient addition only increased CH₄ fluxes when N alone was added at the mixed forest
398 (CH₄-Treatment: $F_{3,24} = 18.79$, $P < 0.001$) (Fig. 5c). Addition of N, P, and NP did not have a
399 significant effect on the fluxes of CH₄ at the palm swamp, nor on the CO₂ and N₂O fluxes
400 from both vegetation communities (Fig. 5).

401

402 4. Discussion

403 4.1 Variation in CO₂ and CH₄ fluxes due to vegetation communities

404 In our first hypothesis, we set out to test how vegetation communities could potentially
405 influence the magnitude of CO₂ and CH₄ fluxes in coastal tropical peatlands. Our results
406 suggest that, throughout a year, there was no significant difference in the magnitude of the
407 CO₂ and CH₄ fluxes due to the vegetation community (Fig. 1; Table 3). Therefore, the overall
408 CO₂ and CH₄ fluxes, from the peat surface, do not vary between the mixed forest and palm
409 swamp in spite of the physiological differences between the dominant species inhabiting the
410 sites (*i.e.*, *C. panamensis* and *R. taedigera*) (Table S1), particularly the contrasting structure
411 of their root system. It is important to mention that our approach did not measure CH₄
412 transport through the vegetation structures (*e.g.* lenticels, pneumatophores, stems, leaves)
413 which could be potentially different among the distinct tree species (Welch et al., 2019).
414 Indeed, it has been quantified that large quantities of CH₄ are emitted through trees in tropical
415 ecosystems, contributing with up to 58 % of the total CH₄ fluxes from tropical ecosystems
416 (Pangala et al., 2017). Furthermore, it has been reported that roots respiration contributes
417 with up to 49 % of the overall CO₂ flux from the peat surface (Girkin et al., 2018a).

418 Despite the fact that it has been observed that belowground peat is also actively producing
419 CO₂ and CH₄ (Wright et al., 2011), the mean peat depth, varying from 96 ± 7 to 483 ± 98 cm
420 (Table 1), did not provide a reliable predictor for the overall CO₂ and CH₄ gas fluxes from the
421 peat surface. This may be due to the fact that the layers contributing the most to the peat
422 surface CO₂ and CH₄ fluxes correspond to those located in the top 1 m, under water logged
423 conditions (Hoyos-Santillan et al., 2016b; Wright et al., 2011). Consequently, even though
424 CO₂ and CH₄ are produced below the 1 m peat layer, deeper layers contribute to lesser extent
425 to the overall production and do not significantly affect the vertical cumulative flux of these
426 gases. In addition, gas transport mediated by vegetation, including radial oxygen loss through
427 the roots (Hoyos-Santillan et al., 2016a), as well as the release of root exudates (Girkin et al.,

428 2018), are mainly constrained to the upper peat layers in the rhizosphere influence zone, were
429 most of peat's CO₂ and CH₄ are produced.

430 The magnitude of the CO₂ and CH₄ fluxes from the peat surface measured in this study are
431 consistent with those previously reported for peatlands in South East Asia, South America,
432 Central America, Hawaii and the Congo River Basin (Sjögersten et al., 2014). Thus, our
433 fluxes fall within a relatively well constrained range of magnitudes comprising several types
434 of vegetation and different geographical locations. For example, our maximum recorded CO₂
435 fluxes (*i.e.*, 913.18 and 719.94 mg m⁻² h⁻¹) are comparable to those previously reported for
436 Indonesia (950 mg m⁻² h⁻¹) (Hirano et al., 2009), Malaysia (905 mg m⁻² h⁻¹) (Melling et al.,
437 2005), and Brazil (583 mg m⁻² h⁻¹) (Belger et al., 2011). Likewise, our maximum registered
438 CH₄ fluxes (48.89 and 38.78 mg m⁻² h⁻¹) are in the same order of magnitude than the
439 maximum reported for Hawaii (14.17 mg m⁻² h⁻¹) (Grand and Gaidos, 2010), Costa Rica
440 (40.4 mg m⁻² h⁻¹) (Nahlik and Mitsch, 2011), Venezuela (95.3 mg m⁻² h⁻¹) (Smith et al.,
441 2000), and Brazil (47.3 mg m⁻² h⁻¹) (Devol et al., 1990).

442

443 4.2 Influence of water table on CO₂ and CH₄ fluxes

444 With respect to our second hypothesis, predicting higher CO₂ fluxes during the dry season in
445 comparison with the wet season and the opposite for CH₄ fluxes, CO₂ fluxes did suggest an
446 apparent seasonal trend, increasing as monthly precipitation rates decreased (Fig. 1a,b).

447 However, CH₄ fluxes did not show a clear seasonal pattern (Fig. 1c,d). The seasonal trend
448 observed on the CO₂ fluxes has been previously described in other tropical peatlands, with
449 high fluxes being observed during the dry season and relatively lower fluxes occurring during
450 the wet season (Jauhiainen et al., 2005; Wright et al., 2013). This trend is related to the
451 decrease of the water table level during low precipitation periods, exposing recently produced

452 organic matter (*e.g.* litter and root exudates) and peat to oxic conditions (Baird et al., 2017),
453 under which rapid aerobic decomposition can occur (Hoyos-Santillan et al., 2015). Indeed,
454 water table does directly respond to precipitation, raising several centimeters above the peat
455 surface during heavy rainfall periods (> 30 cm) (Chimner and Ewel, 2004), and dropping
456 below the surface as the precipitation is no longer sufficient to maintain a steady water table
457 level close to or above the surface (Jauhiainen et al., 2005). We did observe higher CO₂
458 fluxes when the water table was located below the surface (Fig. 3a; Table 3). The CO₂ fluxes
459 increased 80 and 51 % at the mixed forest and palm swamp, respectively, as the level of the
460 water table decreased with respect to the peat surface. Such increases in CO₂ fluxes at lower
461 water tables is plausibly linked to increased activity of the bacteria community or a shift in
462 abundance of the microbial community, *e.g.* towards gram positive bacteria, which are more
463 abundant in surface peat (Dhandapani et al., 2018; Jackson et al., 2009).

464 CH₄ fluxes did not present a clear seasonal trend associated with precipitation rates (Fig.
465 1c,d), this has been reported in other tropical peatlands (Wright et al., 2013), in association
466 with a highly variable fluxes as the ones observed in this study. However, we did observe
467 higher CH₄ fluxes when the water table was above the surface in comparison to those fluxes
468 when the water table was located below the surface (Fig. 3b; Table 3). Methane fluxes were
469 39 and 81 % higher at the mixed forest and palm swamp, respectively, when the water table
470 was located above the peat surface compared to when the water table was below the peat
471 surface. This is due to the anoxic conditions being promoted by high water table levels,
472 functioning as a barrier for oxygen transfer from the atmosphere to the peat matrix,
473 facilitating methanogenesis (Sepulveda-Jauregui et al., 2018) (Fig. 3b. Table 3). Thus, our
474 results are consistent with previous research indicating that the level of the water table with
475 respect to the peat surface is among the main drivers controlling greenhouse gases fluxes
476 (Cobb et al., 2017; Couwenberg et al., 2011; Hirano et al., 2009; Jauhiainen et al., 2005).

477 It is important to consider that, the water table level is directly related to the type of
478 vegetation that is currently producing or produced the peat, the stratigraphic structure
479 defining the hydraulic properties of peat (Couwenberg and Joosten, 1999; Joosten and Clarke,
480 2002), and the regional precipitation rates. Our results suggest that, the vegetation at the
481 mixed forest and the palm swamp exert an overall equivalent effect on the water table and
482 peat properties, creating similar conditions for greenhouse gases emissions in both vegetation
483 communities. Nevertheless, microtopography can promote strong fluctuations of the water
484 table levels during the same day at the same area (Lampela et al., 2014), potentially affecting
485 CO₂ and CH₄ fluxes in relatively short periods of time. It is necessary that new and larger
486 data sets of greenhouse gas fluxes are produced, considering the water table fluctuations, in
487 order to reduce the uncertainty of the current greenhouse gas budgets from tropical peatlands.
488 Furthermore, since greenhouse gas emissions transported through vegetation were not
489 measured in this study, it is important that future studies explore the contribution of such
490 fluxes to the overall emissions in different ecosystems, as well as exploring the interaction
491 between the water table level and the tree mediated transport (*e.g.*, effect of water table on
492 pneumatophores and lenticels functioning) (Welch et al., 2019).

493

494 4.3 Peat composition effect on CO₂ and CH₄ fluxes

495 In our evaluation of our third hypotheses, testing how peat composition could potentially
496 affect CO₂ and CH₄ fluxes (*i.e.* C:N ratio; peat content of lignin, short and long fatty acids,
497 and phenolic compounds), only the content of long fatty acids moderately influenced CH₄
498 fluxes (Table S4). This is related to the origin of the main substrates contributing to produce
499 CO₂ and CH₄ in peat. For example, readily decomposable compounds such as root exudates
500 (*i.e.*, young carbon) (Couwenberg and Fritz, 2012; N.T. Girkin et al., 2018; Segers, 1998) and

501 compounds derived from recently fallen litter (Hoyos-Santillan et al., 2016b) are the most
502 important carbon sources for heterotrophic microbial communities involved in methanogenic
503 pathways. Regarding the abundance of lignin moieties in the surface peat, sites dominated by
504 *R. taedigera* have been reported to have higher content of *p*-coumaryl alcohol than sites
505 dominated by *C. panamensis*, and sites dominated by *C. panamensis* have a higher content of
506 coniferyl and sinapyl alcohols (Hoyos-Santillan et al., 2016b). This is due to the fact that
507 monocotyledonous angiosperms (*e.g.*, *R. taedigera* palms), develop hydroxyl phenol-
508 guaiacyl-syringyl lignin (Ek et al., 2009), whilst dicotyledonous trees (*e.g.*, *C. panamensis*
509 hardwood tree) develop syringyl-guaiacyl lignin, rich in coniferyl alcohol (Ek et al., 2009).
510 These differences contribute to define the recalcitrance of peat; for example, hardwood lignin
511 is more resistant to decomposition (Vancampenhout et al., 2008) than phenol-guaiacyl-
512 syringyl lignin. However, lignin content was not a good predictor for CO₂ or CH₄ gas fluxes.
513 Rapid decomposition of old peat mainly occurs if water table draws down (*e.g.*, peat
514 drainage), for a period of time long enough for oxic conditions to be established (Hooijer et
515 al., 2012). However, under waterlogged conditions, the less recalcitrant organic matter
516 remains as the main substrate for CO₂ and CH₄ production (Hoyos-Santillan et al., 2016b).
517 Consequently, in order to maintain the stability of old peat, (> 5000 years old in the study
518 area), all factors necessary to maintain a high water table, such as the input of autochthonous
519 vegetation litter, constant input of water, and the stability of the peat structure at top layers
520 must be preserved.

521

522 4.4 Nutrient addition impact on CO₂, CH₄, and N₂O fluxes

523 Regarding our fourth hypothesis, predicting that the addition of N and P to the peat would
524 increase CO₂ CH₄, and N₂O fluxes, our data showed that only the individual addition of

525 nitrogen increased CH₄ fluxes in the mixed forest (Fig. 5c). The increase in CH₄ fluxes as
526 response to N addition has been previously reported for several ecosystems (Banger et al.,
527 2012; Liu and Greaver, 2009), and has been related to alterations on the methanogenesis and
528 methanotrophy rates. Indeed, the balance between these two processes, occurring
529 simultaneously in soil, determines the net CH₄ emission (Aerts and Toet, 1997; Schnell and
530 King, 1994). The mechanisms that have been associated to an increase in CH₄ emissions due
531 to N addition are related to the inhibition of methanotrophy and the enhancement of
532 methanogenesis (Banger et al., 2012). For example, in our experiment, it is plausible that the
533 following mechanisms, inhibiting CH₄ oxidation in peat, were responsible for the net increase
534 of CH₄ emission following N addition at the mixed forest: i) competitive inhibition of
535 methane monooxygenase (MOO) by ammonium (NH₄⁺) (Bédard and Knowles, 1989), and ii)
536 toxicity of nitrite (NO₂⁻), which is the end product of methanotrophic ammonia oxidation, to
537 methanotrophs (Schnell and King, 1994). The addition of P or NP did not significantly
538 influence CO₂, CH₄, or N₂O fluxes. Consistently with the seasonal monitoring experiment,
539 the water table played a major role as driver of greenhouse gas fluxes. The CO₂ fluxes were
540 significantly higher when the water table was located below the water surface at the palm
541 swamp, whereas higher CH₄ fluxes were observed when the water table was above peat
542 surface at the mixed forest (Fig. 3). Since the water table has such a strong effect on the
543 magnitude of the fluxes, it is possible that the controls posed by the water table had cancelled
544 out, to some extent, the effect related to the vegetation community or nutrient addition. The
545 higher fluxes of N₂O observed with low water table are explained by the dependency of N₂O
546 production with the oxic-anoxic conditions in the peat. As the water table drops, ammonia is
547 oxidized through nitrification producing NO₂⁻ and NO₃⁻; NO₂⁻ is then reduced under
548 microaerophilic conditions in areas of the peat matrix with 70 – 80 % of moisture saturation
549 releasing as one of the byproducts N₂O (Butterbach-Bahl et al., 2013). Thus, the fluctuation

550 of the water table may work as a two stage system that, during the low level conditions,
551 produces the substrates that are precursors for N₂O once the water table rises. The average
552 N₂O fluxes at the mixed forest and the palm swamp (mixed forest: $0.018 \pm 0.005 \text{ mg m}^{-2} \text{ h}^{-1}$;
553 palm swamp: $0.206 \pm 0.012 \text{ mg m}^{-2} \text{ h}^{-1}$) are in the same order of magnitude of those reported
554 for pristine and anthropogenically impacted palm swamps in the region (pristine: $0.06 \pm$
555 $0.008 \text{ mg m}^{-2} \text{ h}^{-1}$; anthropogenically impacted: $0.09 \pm 0.015 \text{ mg m}^{-2} \text{ h}^{-1}$) (Hoyos-Santillan et
556 al., 2016a).

557 Alternatively, it is plausible that the addition of nutrients did not influence the greenhouse gas
558 fluxes because the system was not limited by N or P, but was limited by the availability of
559 easily degradable organic matter that could be used for the heterotrophic processes involved
560 in the different gas production pathways. Indeed, nutrient addition does not affect litter
561 decomposition in this ecosystems either (Hoyos-Santillan et al., 2018).

562

563 4.5 Implications for the estimation of CO₂ and CH₄ fluxes on a regional scale

564 The type of vegetation currently inhabiting the studied peatlands, the mean peat depth, the
565 peat composition and the nutrient availability did not represent good predictors of the overall
566 fluxes of CO₂ and CH₄ from the peat surface. As consequence, our results suggest that
567 discrimination among vegetation communities does not represent a relevant aspect when
568 developing projections of CO₂ or CH₄ emissions from the surface of tropical forested
569 peatlands. This is important when developing projections of carbon budgets by using remote
570 sensing approaches (top-down), for it would be possible to include all types of forested
571 peatlands into one category rather than developing thorough vegetation surveys. It is
572 important to consider that our estimations do not consider the emissions transported through
573 vegetation. Evaluating such contribution would require further studies on the specific

574 capacity of gas conduction by different plant species. However, in line with literature, the
575 water table level was one of the main drivers controlling greenhouse gas emissions in the
576 studied ecosystems (Couwenberg et al., 2011; Couwenberg and Fritz, 2012). Therefore, CO₂
577 and CH₄ fluxes in coastal tropical peatlands could potentially be estimated, within a relatively
578 narrow range, if the fluctuation of the water table is measured in a regular basis through
579 satellite or airborne imagery (Bechtold et al., 2018; Kalacska et al., 2018). For example, it has
580 been possible to evaluate the dynamics of water table in temperate peatlands by using the
581 Advance Synthetic Aperture Radar data from ENVISAT and Sentinel satellites (Asmub et al.,
582 2018; Bechtold et al., 2018; Dabrowska-Zielinska et al., 2016). Thus, by reducing uncertainty
583 on the measurements of greenhouse gas fluxes at the peat's surface, and relating them with
584 variables such as the level of the water table, it would be possible to develop better top-down
585 projections, with seasonal resolution, of the carbon fluxes from tropical peatlands.
586 Furthermore, since the CO₂ and CH₄ fluxes were independent from the peat depth, it is not
587 required to measure it in order to develop estimations of the overall greenhouse gas fluxes.
588 Based on our average fluxes, including the distinct positions of the water table (CO₂-above
589 surface: $230.97 \pm 20.56 \text{ mg m}^{-2} \text{ h}^{-1}$, CH₄-above surface: $5.43 \pm 1.75 \text{ mg m}^{-2} \text{ h}^{-1}$; CO₂-below
590 surface: $381.44 \pm 36.85 \text{ mg m}^{-2} \text{ h}^{-1}$, CH₄-below surface: $3.25 \pm 0.46 \text{ mg m}^{-2} \text{ h}^{-1}$), we estimated
591 that the contribution of CH₄ to the overall emissions from the peat surface, accounts for ≈ 20
592 % of the total emissions when the water table is below the surface (expressed as CO₂
593 equivalents (CO_{2eq}; global warming potential value relative to CO₂: CH₄ = 28). This
594 contribution increases, with respect to CO₂, as the fraction of the flooded peatland area
595 increases, potentially reaching 40 % in terms of CO_{2eq}, considering the scenario where water
596 table for the entire peatland is above the surface (Fig. 6). Nevertheless, CO₂ remains the most
597 important contributor to greenhouse gas emissions in these ecosystems under both the non-

598 flooded or completely flooded scenarios, as previously observed in other tropical peatlands
599 (Hergoualc'h and Verchot, 2014; Hirano et al., 2009).

600

601 **5. Conclusions**

602

603 We conclude that the magnitude of the fluxes of CO₂ and CH₄ at the peat surface in forested
604 lowland tropical peatlands is independent of the vegetation communities. However, water
605 table level functions as a strong factor controlling CO₂ and CH₄ fluxes from forested tropical
606 peatlands, with CO₂ and CH₄ fluxes increasing when the water table was below or above the
607 peat surface, respectively. Therefore, the distribution of vegetation communities alone should
608 not be used as a proxy to estimate the magnitude of greenhouse gas emissions. Finally,
609 additional relevance must be given to the development of remote sensing alternatives
610 allowing to monitor the water table in tropical peatlands on a regular basis. This will provide
611 valuable information that will help to predict large fluctuations on the magnitudes of CO₂,
612 CH₄, and N₂O fluxes in these ecosystems.

613

614 **Acknowledgments**

615 J.H.S. thanks The National *Council* on Science and Technology (*CONACyT-Mexico*) for his
616 PhD scholarship (211962). The authors also thank the Light Hawk program for its support in
617 the aerial surveys. We thank Erick Brown for field assistance, and Gabriel Jácome, Plinio
618 Góndola, Dayana Agudo, Tania Romero, Luis A. Ramos, Dianne de la Cruz, Vanessa Pardo,
619 John Corrie and Darren Hepworth for logistical and laboratory support. The authors declare
620 that there are no conflicts of interest.

621 **Data accessibility**

622 Data to support this article is publicly available at Dryad Digital Repository

623

624 **References**

625 Aerts, R., Toet, S., 1997. Nutritional controls on carbon dioxide and methane emission from
626 Carex-dominated peat soils. *Soil Biol. Biochem.* 29, 1683–1690.

627 [https://doi.org/10.1016/S0038-0717\(97\)00073-4](https://doi.org/10.1016/S0038-0717(97)00073-4)

628 Asmub, T., Bechtold, M., Tiemeyer, B., 2018. Towards Monitoring Groundwater Table

629 Depth in Peatlands from Sentinel-1 Radar Data, in: *IGARSS 2018 - 2018 IEEE*

630 International Geoscience and Remote Sensing Symposium. IEEE, pp. 7793–7796.

631 <https://doi.org/10.1109/IGARSS.2018.8518838>

632 Baird, A.J., Low, R., Young, D., Swindles, G.T., Lopez, O.R., Page, S., 2017. High

633 permeability explains the vulnerability of the carbon store in drained tropical peatlands.

634 *Geophys. Res. Lett.* 44, 1333–1339. <https://doi.org/10.1002/2016GL072245>

635 Banger, K., Tian, H., Lu, C., 2012. Do nitrogen fertilizers stimulate or inhibit methane

636 emissions from rice fields? *Glob. Chang. Biol.* 18, 3259–3267.

637 <https://doi.org/10.1111/j.1365-2486.2012.02762.x>

638 Bechtold, M., Schlaffer, S., Tiemeyer, B., De Lannoy, G., 2018. Inferring Water Table Depth

639 Dynamics from ENVISAT-ASAR C-Band Backscatter over a Range of Peatlands from

640 Deeply-Drained to Natural Conditions. *Remote Sens.* 10, 536.

641 <https://doi.org/10.3390/rs10040536>

642 Bédard, C., Knowles, R., 1989. Physiology, biochemistry, and specific inhibitors of CH₄,

643 NH₄⁺, and CO oxidation by methanotrophs and nitrifiers. *Microbiol. Rev.* 53, 68–84.

644 Belger, L., Forsberg, B.R., Melack, J.M., 2011. Carbon dioxide and methane emissions from
645 interfluvial wetlands in the upper Negro River basin, Brazil. *Biogeochemistry* 105, 171–
646 183. <https://doi.org/10.1007/s10533-010-9536-0>

647 Brookes, P.C., Powlson, D.S., Jenkinson, D.S., 1982. Measurement of microbial biomass
648 phosphorus in soil. *Soil Biol. Biochem.* 14, 319–329. [https://doi.org/10.1016/0038-](https://doi.org/10.1016/0038-0717(82)90001-3)
649 [0717\(82\)90001-3](https://doi.org/10.1016/0038-0717(82)90001-3)

650 Butterbach-Bahl, K., Baggs, E.M., Dannenmann, M., Kiese, R., Zechmeister-Boltenstern, S.,
651 2013. Nitrous oxide emissions from soils: how well do we understand the processes and
652 their controls? *Philos. Trans. R. Soc. B Biol. Sci.* 368, 20130122–20130122.
653 <https://doi.org/10.1098/rstb.2013.0122>

654 Chimner, R.A., Ewel, K.C., 2004. Differences in carbon fluxes between forested and
655 cultivated micronesian tropical peatlands. *Wetl. Ecol. Manag.* 12, 419–427.
656 <https://doi.org/10.1007/s11273-004-0255-y>

657 Cobb, A.R., Hoyt, A.M., Gandois, L., Eri, J., Dommain, R., Abu Salim, K., Kai, F.M., Haji
658 Su'ut, N.S., Harvey, C.F., 2017. How temporal patterns in rainfall determine the
659 geomorphology and carbon fluxes of tropical peatlands. *Proc. Natl. Acad. Sci.*
660 201701090. <https://doi.org/10.1073/pnas.1701090114>

661 Cohen, A.D., Raymond, R., Ramirez, A., Morales, Z., Ponce, F., 1989. The Changuinola peat
662 deposit of northwestern Panama: a tropical, back-barrier, peat(coal)-forming
663 environment. *Int. J. Coal Geol.* 12, 157–192. [https://doi.org/10.1016/0166-](https://doi.org/10.1016/0166-5162(89)90050-5)
664 [5162\(89\)90050-5](https://doi.org/10.1016/0166-5162(89)90050-5)

665 Comeau, L.-P., Hergoualc'h, K., Hartill, J., Smith, J., Verchot, L. V., Peak, D., Salim, A.M.,
666 2016. How do the heterotrophic and the total soil respiration of an oil palm plantation on
667 peat respond to nitrogen fertilizer application? *Geoderma* 268, 41–51.

668 <https://doi.org/10.1016/j.geoderma.2016.01.016>

669 Couwenberg, J., Dommain, R., Joosten, H., 2010. Greenhouse gas fluxes from tropical
670 peatlands in south-east Asia. *Glob. Chang. Biol.* 16, 1715–1732.
671 <https://doi.org/10.1111/j.1365-2486.2009.02016.x>

672 Couwenberg, J., Fritz, C., 2012. Towards developing IPCC methane ‘emission factors’ for
673 peatlands (organic soils). *Mires Peat* 10, 1–17.

674 Couwenberg, J., Joosten, H., 1999. Pools as Missing Links: The Role of Nothing in the Being
675 of Mires, in: Standen, V., Tallis, J., Meade, R. (Eds.), *Patterned Mires and Mire Pools-
676 Origin and Development; Flora and Fauna*. British Ecological Society, Durham, pp. 87–
677 102.

678 Couwenberg, J., Thiele, A., Tanneberger, F., Augustin, J., Bärtsch, S., Dubovik, D.,
679 Liashchynskaya, N., Michaelis, D., Minke, M., Skuratovich, A., Joosten, H., 2011.
680 Assessing greenhouse gas emissions from peatlands using vegetation as a proxy.
681 *Hydrobiologia* 674, 67–89. <https://doi.org/10.1007/s10750-011-0729-x>

682 Dabrowska-Zielinska, K., Budzynska, M., Tomaszewska, M., Malinska, A., Gatkowska, M.,
683 Bartold, M., Malek, I., 2016. Assessment of Carbon Flux and Soil Moisture in Wetlands
684 Applying Sentinel-1 Data. *Remote Sens.* 8, 756. <https://doi.org/10.3390/rs8090756>

685 Devol, A.H., Richey, J.E., Forsberg, B.R., Martinelli, L.A., 1990. Seasonal dynamics in
686 methane emissions from the Amazon River floodplain to the troposphere. *J. Geophys.
687 Res.* 95, 16417. <https://doi.org/10.1029/JD095iD10p16417>

688 Dhandapani, S., Ritz, K., Evers, S., Yule, C.M., Sjögersten, S., 2018. Are secondary forests
689 second-rate? Comparing peatland greenhouse gas emissions, chemical and microbial
690 community properties between primary and secondary forests in Peninsular Malaysia.
691 *Sci. Total Environ.* <https://doi.org/10.1016/j.scitotenv.2018.11.046>

692 Dias, A.T.C., Hoorens, B., Van Logtestijn, R.S.P., Vermaat, J.E., Aerts, R., 2010. Plant
693 Species Composition Can Be Used as a Proxy to Predict Methane Emissions in Peatland
694 Ecosystems After Land-Use Changes. *Ecosystems* 13, 526–538.
695 <https://doi.org/10.1007/s10021-010-9338-1>

696 Dommain, R., Couwenberg, J., Glaser, P.H., Joosten, H., Suryadiputra, I.N.N., 2014. Carbon
697 storage and release in Indonesian peatlands since the last deglaciation. *Quat. Sci. Rev.*
698 97, 1–32. <https://doi.org/10.1016/j.quascirev.2014.05.002>

699 Draper, F.C., Roucoux, K.H., Lawson, I.T., Mitchard, E.T.A., Honorio Coronado, E.N.,
700 Lähteenoja, O., Torres Montenegro, L., Valderrama Sandoval, E., Zaráte, R., Baker,
701 T.R., 2014. The distribution and amount of carbon in the largest peatland complex in
702 Amazonia. *Environ. Res. Lett.* 9, 124017. [https://doi.org/10.1088/1748-](https://doi.org/10.1088/1748-9326/9/12/124017)
703 [9326/9/12/124017](https://doi.org/10.1088/1748-9326/9/12/124017)

704 Ek, M., Gellerstedt, G., Henriksson, G., 2009. *Pulp and Paper Chemistry and Technology:*
705 *Wood Chemistry and Wood Biotechnology.* Walter de Gruyter, Berlin.
706 <https://doi.org/10.1515/9783110213409>

707 Feller, I.C., 1995. Effects of Nutrient Enrichment on Growth and Herbivory of Dwarf Red
708 Mangrove (*Rhizophora Mangle*). *Ecol. Monogr.* 65, 477.
709 <https://doi.org/10.2307/2963499>

710 Girkin, N.T., Turner, B.L., Ostle, N., Craigon, J., Sjögersten, S., 2018. Root exudate
711 analogues accelerate CO₂ and CH₄ production in tropical peat. *Soil Biol. Biochem.* 117,
712 48–55. <https://doi.org/10.1016/j.soilbio.2017.11.008>

713 Girkin, N T, Turner, B.L., Ostle, N., Sjögersten, S., 2018a. Root-derived CO₂ flux from a
714 tropical peatland. *Wetl. Ecol. Manag.* <https://doi.org/10.1007/s11273-018-9617-8>

715 Girkin, N T, Vane, C.H., Cooper, H. V., Moss-Hayes, V., Craigon, J., Turner, B.L., Ostle, N.,

716 Sjögersten, S., 2018b. Spatial variability of organic matter properties determines
717 methane fluxes in a tropical forested peatland. *Biogeochemistry*.
718 <https://doi.org/10.1007/s10533-018-0531-1>

719 Grand, M., Gaidos, E., 2010. Methane Emission from a Tropical Wetland in Ka'au Crater,
720 O'ahu, Hawai'i 1. *Pacific Sci.* 64, 57–72. <https://doi.org/10.2984/64.1.057>

721 Hergoualc'h, K., Verchot, L. V., 2014. Greenhouse gas emission factors for land use and
722 land-use change in Southeast Asian peatlands. *Mitig. Adapt. Strateg. Glob. Chang.* 19,
723 789–807. <https://doi.org/10.1007/s11027-013-9511-x>

724 Hirano, T., Jauhiainen, J., Inoue, T., Takahashi, H., 2009. Controls on the carbon balance of
725 tropical peatlands. *Ecosystems* 12, 873–887. <https://doi.org/10.1007/s10021-008-9209-1>

726 Hooijer, A., Page, S., Jauhiainen, J., Lee, W.A., Lu, X.X., Idris, A., Anshari, G., 2012.
727 Subsidence and carbon loss in drained tropical peatlands. *Biogeosciences* 9, 1053–1071.
728 <https://doi.org/10.5194/bg-9-1053-2012>

729 Houghton, R., 2012. Carbon emissions and the drivers of deforestation and forest
730 degradation in the tropics. *Curr. Opin. Environ. Sustain.* 4, 597–603.
731 <https://doi.org/10.1016/j.cosust.2012.06.006>

732 Hoyos-Santillan, J., 2014. Controls of carbon turnover in lowland tropical peatlands. The
733 University of Nottingham. <https://doi.org/10.13140/2.1.3387.2329>

734 Hoyos-Santillan, J., Craigon, J., Lomax, B.H., Lopez, O.R., Turner, B.L., Sjögersten, S.,
735 2016a. Root oxygen loss from *Raphia taedigera* palms mediates greenhouse gas
736 emissions in lowland neotropical peatlands. *Plant Soil* 404, 47–60.
737 <https://doi.org/10.1007/s11104-016-2824-2>

738 Hoyos-Santillan, J., Lomax, B.H., Large, D., Turner, B.L., Boom, A., Lopez, O.R.,
739 Sjögersten, S., 2016b. Quality not quantity: Organic matter composition controls of CO₂

740 and CH₄ fluxes in neotropical peat profiles. *Soil Biol. Biochem.* 103, 86–96.
741 <https://doi.org/10.1016/j.soilbio.2016.08.017>

742 Hoyos-Santillan, J., Lomax, B.H., Large, D., Turner, B.L., Boom, A., Lopez, O.R.,
743 Sjögersten, S., 2015. Getting to the root of the problem: litter decomposition and peat
744 formation in lowland Neotropical peatlands. *Biogeochemistry* 126, 115–129.
745 <https://doi.org/10.1007/s10533-015-0147-7>

746 Hoyos-Santillan, J., Lomax, B.H., Turner, B.L., Sjögersten, S., 2018. Nutrient limitation or
747 home field advantage: Does microbial community adaptation overcome nutrient
748 limitation of litter decomposition in a tropical peatland? *J. Ecol.* 106, 1558–1569.
749 <https://doi.org/10.1111/1365-2745.12923>

750 Jackson, C.R., Liew, K.C., Yule, C.M., 2009. Structural and Functional Changes with Depth
751 in Microbial Communities in a Tropical Malaysian Peat Swamp Forest. *Microb. Ecol.*
752 57, 402–412. <https://doi.org/10.1007/s00248-008-9409-4>

753 Järveoja, J., Peichl, M., Maddison, M., Soosaar, K., Vellak, K., Karofeld, E., Teemusk, A.,
754 Mander, Ü., 2016. Impact of water table level on annual carbon and greenhouse gas
755 balances of a restored peat extraction area. *Biogeosciences* 13, 2637–2651.
756 <https://doi.org/10.5194/bg-13-2637-2016>

757 Jauhiainen, J., Takahashi, H., Heikkinen, J.E.P., Martikainen, P.J., Vasander, H., 2005.
758 Carbon fluxes from a tropical peat swamp forest floor. *Glob. Chang. Biol.* 11, 1788–
759 1797. <https://doi.org/10.1111/j.1365-2486.2005.001031.x>

760 Joosten, H., Clarke, D., 2002. *Wise Use of Mires and Peatlands: Background and Principles*
761 *including a Framework for Decision-Making.* International Mire Conservation Group
762 and International Peat Society, Saarijärvi, Finland.

763 Kalacska, M., Arroyo-Mora, J., Soffer, R., Roulet, N., Moore, T., Humphreys, E., Leblanc,

764 G., Lucanus, O., Inamdar, D., 2018. Estimating Peatland Water Table Depth and Net
765 Ecosystem Exchange: A Comparison between Satellite and Airborne Imagery. *Remote*
766 *Sens.* 10, 687. <https://doi.org/10.3390/rs10050687>

767 Khalil, M.I., Rahman, M.S., Schmidhalter, U., Olf, H.-W., 2007. Nitrogen fertilizer-induced
768 mineralization of soil organic C and N in six contrasting soils of Bangladesh. *J. Plant*
769 *Nutr. Soil Sci.* 170, 210–218. <https://doi.org/10.1002/jpln.200520534>

770 Kirschke, S., Bousquet, P., Ciais, P., Saunoy, M., Canadell, J.G., Dlugokencky, E.J.,
771 Bergamaschi, P., Bergmann, D., Blake, D.R., Bruhwiler, L., Cameron-Smith, P.,
772 Castaldi, S., Chevallier, F., Feng, L., Fraser, A., Heimann, M., Hodson, E.L.,
773 Houweling, S., Josse, B., Fraser, P.J., Krummel, P.B., Lamarque, J.-F., Langenfelds,
774 R.L., Le Quéré, C., Naik, V., O'Doherty, S., Palmer, P.I., Pison, I., Plummer, D.,
775 Poulter, B., Prinn, R.G., Rigby, M., Ringeval, B., Santini, M., Schmidt, M., Shindell,
776 D.T., Simpson, I.J., Spahni, R., Steele, L.P., Strode, S.A., Sudo, K., Szopa, S., van der
777 Werf, G.R., Voulgarakis, A., van Weele, M., Weiss, R.F., Williams, J.E., Zeng, G.,
778 2013. Three decades of global methane sources and sinks. *Nat. Geosci.* 6, 813–823.
779 <https://doi.org/10.1038/ngeo1955>

780 Lampela, M., Jauhiainen, J., Vasander, H., 2014. Surface peat structure and chemistry in a
781 tropical peat swamp forest. *Plant Soil* 382, 329–347. [https://doi.org/10.1007/s11104-](https://doi.org/10.1007/s11104-014-2187-5)
782 [014-2187-5](https://doi.org/10.1007/s11104-014-2187-5)

783 Lawson, I.T., Kelly, T.J., Aplin, P., Boom, A., Dargie, G., Draper, F.C.H., Hassan,
784 P.N.Z.B.P., Hoyos-Santillan, J., Kaduk, J., Large, D., Murphy, W., Page, S.E., Roucoux,
785 K.H., Sjögersten, S., Tansey, K., Waldram, M., Wedeux, B.M.M., Wheeler, J., 2015.
786 Improving estimates of tropical peatland area, carbon storage, and greenhouse gas
787 fluxes. *Wetl. Ecol. Manag.* 23, 327–346. <https://doi.org/10.1007/s11273-014-9402-2>

788 Leifeld, J., Menichetti, L., 2018. The underappreciated potential of peatlands in global
789 climate change mitigation strategies. *Nat. Commun.* 9, 1071.
790 <https://doi.org/10.1038/s41467-018-03406-6>

791 Liu, L., Greaver, T.L., 2009. A review of nitrogen enrichment effects on three biogenic
792 GHGs: the CO₂ sink may be largely offset by stimulated N₂O and CH₄ emission. *Ecol.*
793 *Lett.* 12, 1103–1117. <https://doi.org/10.1111/j.1461-0248.2009.01351.x>

794 Melling, L., Hatano, R., Goh, K.J., 2005. Soil CO₂ flux from three ecosystems in tropical
795 peatland of Sarawak, Malaysia. *Tellus, Ser. B Chem. Phys. Meteorol.* 57, 1–11.
796 <https://doi.org/10.1111/j.1600-0889.2005.00129.x>

797 Myers, R.G., Thien, S.J., Pierzynski, G.M., 1999. Using an Ion Sink to Extract Microbial
798 Phosphorus from Soil. *Soil Sci. Soc. Am. J.* 63, 1229.
799 <https://doi.org/10.2136/sssaj1999.6351229x>

800 Myers, R.L., 1981. The ecology of low diversity palm swamps near Tortuguero, Costa Rica.
801 University of Florida.

802 Nahlik, A.M., Mitsch, W.J., 2011. Methane emissions from tropical freshwater wetlands
803 located in different climatic zones of Costa Rica. *Glob. Chang. Biol.* 17, 1321–1334.
804 <https://doi.org/10.1111/j.1365-2486.2010.02190.x>

805 Oktarita, S., Hergoualc'h, K., Anwar, S., Verchot, L. V., 2017. Substantial N₂O emissions
806 from peat decomposition and N fertilization in an oil palm plantation exacerbated by
807 hotspots. *Environ. Res. Lett.* 12, 104007. <https://doi.org/10.1088/1748-9326/aa80f1>

808 Page, S.E., Rieley, J.O., Banks, C.J., 2011. Global and regional importance of the tropical
809 peatland carbon pool. *Glob. Chang. Biol.* 17, 798–818. [https://doi.org/10.1111/j.1365-](https://doi.org/10.1111/j.1365-2486.2010.02279.x)
810 [2486.2010.02279.x](https://doi.org/10.1111/j.1365-2486.2010.02279.x)

811 Pangala, S., Moore, S., Hornibrook, E.R.C., Gauci, V., 2013. Trees are major conduits for

812 methane egress from tropical forested wetlands. *New Phytol.* 197, 524–31.
813 <https://doi.org/10.1111/nph.12031>

814 Pangala, S.R., Enrich-Prast, A., Basso, L.S., Peixoto, R.B., Bastviken, D., Hornibrook,
815 E.R.C., Gatti, L. V., Ribeiro, H., Calazans, L.S.B., Sakuragui, C.M., Bastos, W.R.,
816 Malm, O., Gloor, E., Miller, J.B., Gauci, V., 2017. Large emissions from floodplain
817 trees close the Amazon methane budget. *Nature*. <https://doi.org/10.1038/nature24639>

818 Pearson, T.R.H., Brown, S., Murray, L., Sidman, G., 2017. Greenhouse gas emissions from
819 tropical forest degradation: an underestimated source. *Carbon Balance Manag.* 12, 3.
820 <https://doi.org/10.1186/s13021-017-0072-2>

821 Phillips, S., Rouse, G.E.G., Bustin, R.M., 1997. Vegetation zones and diagnostic pollen
822 profiles of a coastal peat swamp, Bocas del Toro, Panamá. *Palaeogeogr. Palaeoclimatol.*
823 *Palaeoecol.* 128, 301–338. [https://doi.org/10.1016/S0031-0182\(97\)81129-7](https://doi.org/10.1016/S0031-0182(97)81129-7)

824 Schellekens, J., 2013. The use of molecular chemistry (pyrolysis-GC/MS) in the
825 environmental interpretation of peat. Wageningen University.

826 Schnell, S., King, G.M., 1994. Mechanistic analysis of ammonium inhibition of atmospheric
827 methane consumption in forest soils. *Appl. Environ. Microbiol.* 60, 3514–3521.

828 Segers, R., 1998. Methane production and methane consumption: a review of processes
829 underlying wetland methane fluxes. *Biogeochemistry* 41, 23–51.

830 Sepulveda-Jauregui, A., Hoyos-Santillan, J., Martinez-Cruz, K., Walter Anthony, K.M.,
831 Casper, P., Belmonte-Izquierdo, Y., Thalasso, F., 2018. Eutrophication exacerbates the
832 impact of climate warming on lake methane emission. *Sci. Total Environ.* 636, 411–419.
833 <https://doi.org/10.1016/j.scitotenv.2018.04.283>

834 Sjögersten, S., Black, C.R., Evers, S., Hoyos-Santillan, J., Wright, E.L., Turner, B.L., 2014.
835 Tropical wetlands: A missing link in the global carbon cycle? *Global Biogeochem.*

836 Cycles 28. <https://doi.org/10.1002/2014GB004844>

837 Sjögersten, S., Cheesman, A.W., Lopez, O., Turner, B.L., 2011. Biogeochemical processes
838 along a nutrient gradient in a tropical ombrotrophic peatland. *Biogeochemistry* 104,
839 147–163. <https://doi.org/10.1007/s10533-010-9493-7>

840 Smith, L.K., Lewis, W.M., Jeffrey, P., Cronin, G., Hamilton, S.K., 2000. Methane emissions
841 from the Orinoco River floodplain , Venezuela. *Current* 113–140.

842 Steward, C.E., Neff, J., Raab, T.K., Kramer, M., Amatangelo, K., Vitousek, P.M., 2009. Soil
843 organic carbon characterization by pyrolysis-gas chromatography-mass spectrometry
844 (py-GC/MS) and tetramethylammonium-py-GC/MS: Tracing plant and microbial
845 contributions to SOM, in: Marín-Spiotta, E., Cusack, D. (Eds.), 94th ESA Annual
846 Convention: Advances in Biochemical Methods for Studying Organic Matter Dynamics
847 in an Ecological Context. Albuquerque, New Mexico.

848 Teh, Y.A., Murphy, W.A., Berrio, J.-C., Boom, A., Page, S.E., 2017. Seasonal variability in
849 methane and nitrous oxide fluxes from tropical peatlands in the western Amazon basin.
850 *Biogeosciences* 14, 3669–3683. <https://doi.org/10.5194/bg-14-3669-2017>

851 Tian, H., Lu, C., Ciais, P., Michalak, A.M., Canadell, J.G., Saikawa, E., Huntzinger, D.N.,
852 Gurney, K.R., Sitch, S., Zhang, B., Yang, J., Bousquet, P., Bruhwiler, L., Chen, G.,
853 Dlugokencky, E., Friedlingstein, P., Melillo, J., Pan, S., Poulter, B., Prinn, R., Saunio,
854 M., Schwalm, C.R., Wofsy, S.C., 2016. The terrestrial biosphere as a net source of
855 greenhouse gases to the atmosphere. *Nature* 531, 225–228.
856 <https://doi.org/10.1038/nature16946>

857 Troxler, T.G., Ikenaga, M., Scinto, L., Boyer, J.N., Condit, R., Perez, R., Gann, G.D.,
858 Childers, D.L., 2012. Patterns of Soil Bacteria and Canopy Community Structure
859 Related to Tropical Peatland Development. *Wetlands* 32, 769–782.

860 <https://doi.org/10.1007/s13157-012-0310-z>

861 Turetsky, M.R., Benscoter, B., Page, S., Rein, G., van der Werf, G.R., Watts, A., 2014.

862 Global vulnerability of peatlands to fire and carbon loss. *Nat. Geosci.* 8, 11–14.

863 <https://doi.org/10.1038/ngeo2325>

864 Turner, B.L., Romero, T.E., 2009. Short-Term Changes in Extractable Inorganic Nutrients

865 during Storage of Tropical Rain Forest Soils. *Soil Sci. Soc. Am. J.* 73, 1972.

866 <https://doi.org/10.2136/sssaj2008.0407>

867 Urquhart, G.R., 1999. Long-term persistence of *Raphia taedigera* Mart. swamps in Nicaragua.

868 *Biotropica* 31, 565–569. <https://doi.org/10.1111/j.1744-7429.1999.tb00403.x>

869 Vancampenhout, K., Wouters, K., Caus, A., Buurman, P., Swennen, R., Deckers, J., 2008.

870 Fingerprinting of soil organic matter as a proxy for assessing climate and vegetation

871 changes in last interglacial palaeosols (Veldwezelt, Belgium). *Quat. Res.* 69, 145–162.

872 <https://doi.org/10.1016/j.yqres.2007.09.003>

873 Vance, E.D., Brookes, P.C., Jenkinson, D.S., 1987. An extraction method for measuring soil

874 microbial biomass C. *Soil Biol. Biochem.* 19, 703–707. [https://doi.org/10.1016/0038-](https://doi.org/10.1016/0038-0717(87)90052-6)

875 [0717\(87\)90052-6](https://doi.org/10.1016/0038-0717(87)90052-6)

876 VSN International, 2011. GenStat for Windows 14th Edition.

877 Welch, B., Gauci, V., Sayer, E.J., 2019. Tree stem bases are sources of CH₄ and N₂O in a

878 tropical forest on upland soil during the dry to wet season transition. *Glob. Chang. Biol.*

879 25, 361–372. <https://doi.org/10.1111/gcb.14498>

880 Wright, E., Black, C.R., Cheesman, A.W., Drage, T., Large, D., Turner, B.L., Sjögersten, S.,

881 2011. Contribution of subsurface peat to CO₂ and CH₄ fluxes in a neotropical peatland.

882 *Glob. Chang. Biol.* 17, 2867–2881. <https://doi.org/10.1111/j.1365-2486.2011.02448.x>

883 Wright, E.L., Black, C.R., Turner, B.L., Sjögersten, S., 2013. Environmental controls of
 884 temporal and spatial variability in CO₂ and CH₄ fluxes in a neotropical peatland. *Glob.*
 885 *Chang. Biol.* 19, 3775–3789. <https://doi.org/10.1111/gcb.12330>

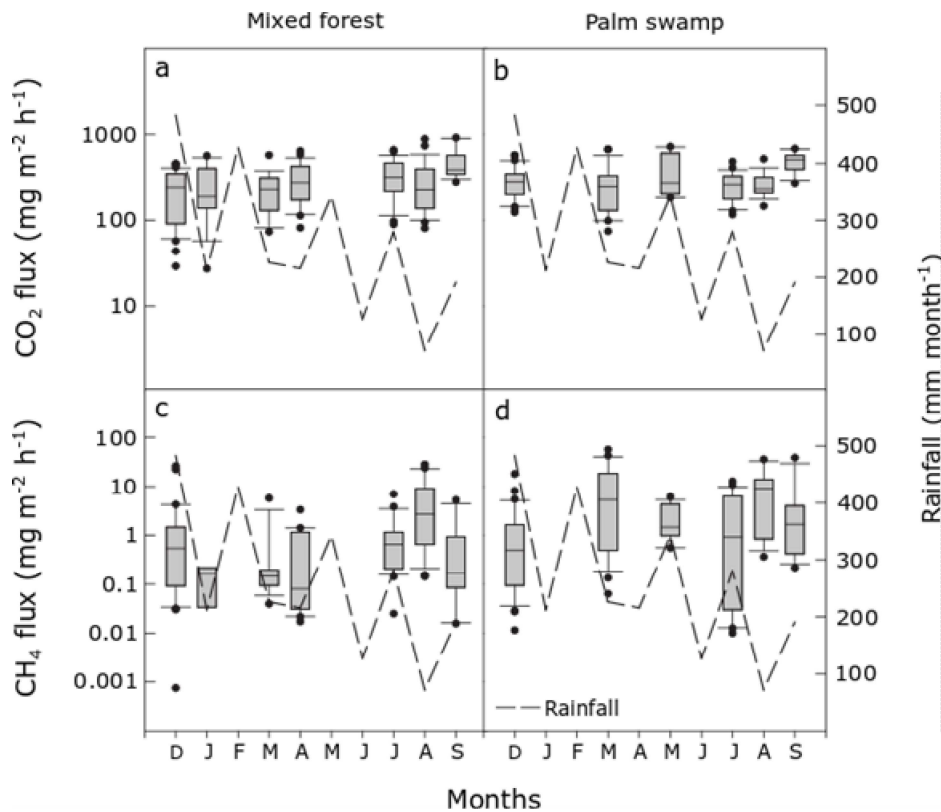
886 Yip, D.Z., Veach, A.M., Yang, Z.K., Cregger, M.A., Schadt, C.W., 2018. Methanogenic
 887 Archaea dominate mature heartwood habitats of Eastern Cottonwood (*Populus deltoides*
 888). *New Phytol.* <https://doi.org/10.1111/nph.15346>

889

890 **Figures and tables captions**

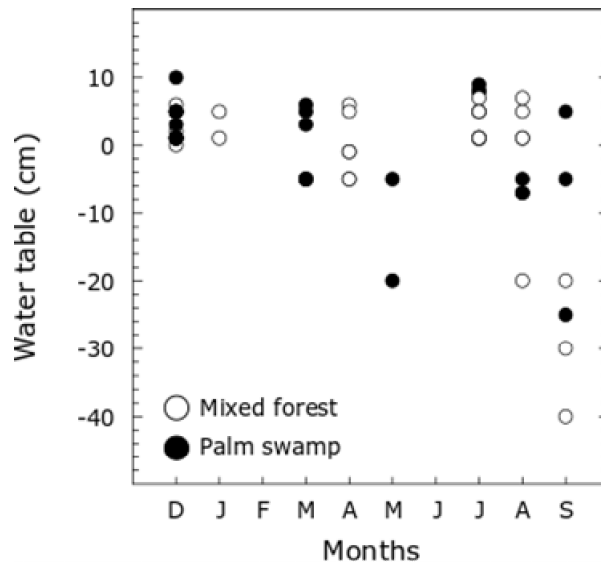
891

892 **Fig. 1** Greenhouse gas fluxes across an annual cycle: CO₂ (a,b) and CH₄ (c,d) fluxes at the
 893 mixed (a,c) forest and palm swamp (b,d). Dash line represents cumulative monthly
 894 precipitation. Relevant statistics are presented in Table 3.



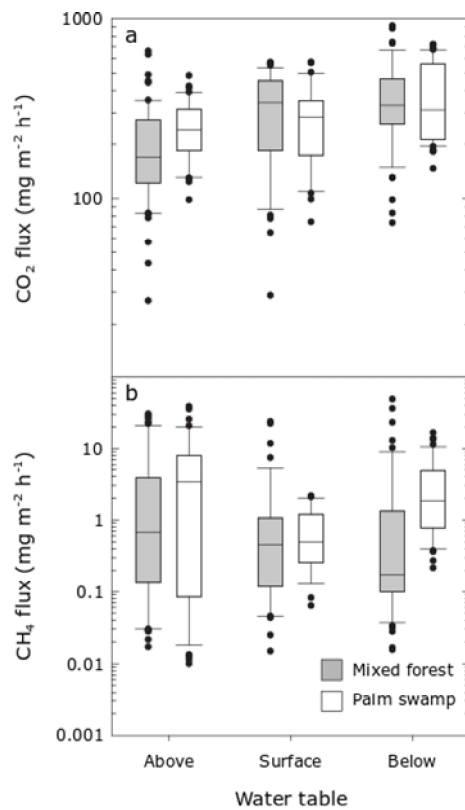
895

896 **Fig. 2** Water table level at all sites during the annual monitoring period. Open and closed
 897 circles correspond to mixed forest (○) and swamp sites (●), respectively.



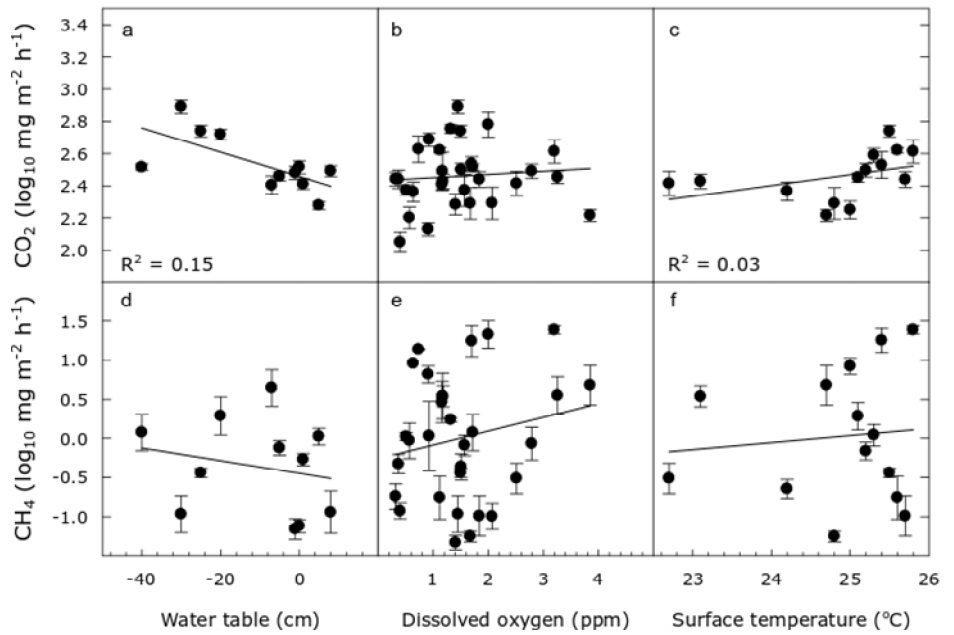
898

899 **Fig. 3** Effect of water table position (above, at, and below the surface) on CO₂ (a) and CH₄
 900 (b) fluxes at the mixed forest (grey boxes) and palm swamp (white boxes) sites. Relevant
 901 statistics are presented in Table 3.



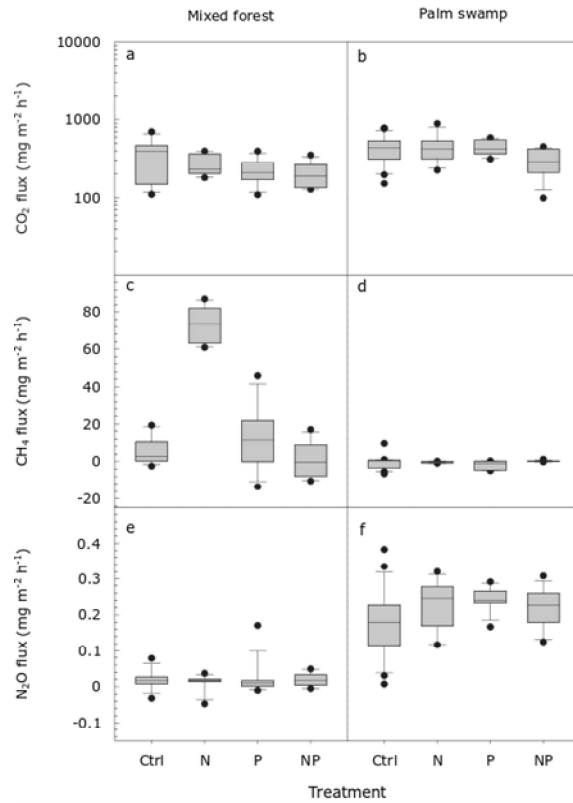
902

903 **Fig. 4** Regression analyses between greenhouse fluxes (CO_2 (a,b,c) and CH_4 (d,e,f)) and *in*
 904 *situ* parameters (water table level, dissolved oxygen in top 0.5 m, and peat's surface
 905 temperature). Symbols represent mean \pm SE. Variance accounted by the model is reported as
 906 the adjusted R^2 within the figures; a summary of the statistical information regarding the
 907 regressions analyses is presented in Table S4.



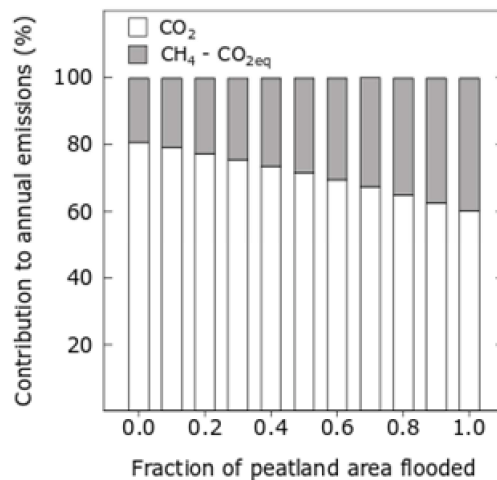
908

909 **Fig. 5** Effect of control (Ctrl), nitrogen (N), phosphorus (P), and nitrogen+phosphorus (NP)
 910 treatment on CO_2 (a,b), CH_4 (c,d), and N_2O (e,f) fluxes at the mixed forest (a,c,e) and palm
 911 swamp (b,d,f). Statistical analyses are presented in the text.



912

913 **Fig. 6** Relative contribution of CO₂ (white bars) and CH₄ (grey bars) to the overall annual
 914 emissions as function of the percentage of flooded area. CH₄ contribution is presented as CO₂
 915 equivalents (CO_{2eq}; CO₂:CH₄ GWP = 28). Calculations are based on the mean greenhouse
 916 gas fluxes under the distinct flooding scenarios (water table above and below the peat's
 917 surface).



918

919

920 **Table 1.** Location and characteristics of study sites.

Table 1. Location and characteristics of study sites

Site	Coordinates	Distance to coast (m)	Phasic community	% basal area (m ² ha ⁻¹)	Peat depth (cm) ^c	¹⁴ C (yr B.P.)
1 Chiriquí Grande	8°58'28.22"N, 82°07'52.85"W	140	Palm swamp	88.3	96 ± 7	-
2 Cricamola River	8°57'17.70"N, 81°54'41.35"W	1400	Palm swamp	70.9	316 ± 37	-
3 San San Pond Sak 1 ^a	9°25'29.20"N, 82°24'05.60"W	500	Palm swamp	98.9	187 ± 5	-
4 San San Pond Sak 2 ^b	9°25'15.00"N, 82°24'14.64"W	1000	Mixed forest	38.7	362 ± 19	3,040 ± 80 ^d
5 Damani-Guariviara	8°57'02.34"N, 81°49'32.40"W	518	Mixed forest	31.6	483 ± 98	5,100 ± 40 ^e
6 Almirante Bay	9°18'17.46"N, 82°21'07.14"W	200	Mixed forest	29.5	165 ± 15	-

^{a,b} San San Pond Sak sites 1 and 2 correspond to sites 1 and 2, respectively, from Sjögersten et al. (2011). Nutrient addition experiment was conducted in these sites

^c Peat definition: 30 % of dry weight organic matter (Joosten and Clarke 2002). Depths correspond to the mean values recorded when peat cores were collected and do not reflect the overall depth in the sites (mean ± SE, n = 3)

^d Data from Phillips and Bustin (1996); the maximum age of the deposit is estimated between 4,000 to 4,500 yr

^e Accelerator mass spectrometer (AMS) dating Beta-300182; Cal BP ± 2 σ = 5,920 to 5,740 (Hoyos-Santillan 2014). Peat sample from 6 m depth

921 **Table 2.** Physicochemical characteristics of peat from the top 10 cm layer.

Table 2. Physicochemical characteristics of peat from the top 10 cm layer 922

Site	pH	Conductivity $\mu\text{S cm}^{-1}$	Bulk Density g cm^{-3}	Loss on ignition %	Total elements			
					C mgC g^{-1}	N mgN g^{-1}	S mgS g^{-1}	P $\mu\text{gP g}^{-1}$
Chiriqui Grande	4.79 ± 0.08	142 ± 26	$0.06 \pm \text{na}$	88.5 ± 2.8	356 ± 120	12.7 ± 5.3	3.9 ± 1.6	$476 \pm \text{na}$
Cricamola River	5.52 ± 0.75	108 ± 15	$0.13 \pm \text{na}$	71.9 ± 9.4	458 ± 250	22.9 ± 18.2	4.7 ± 1.6	$216 \pm \text{na}$
San San Pond Sak 1 ^a	5.05 ± 0.23	64 ± 50	$0.11 \pm \text{na}$	91.7 ± 2.3	502 ± 200	12.1 ± 5.5	1.3 ± 0.7	$267 \pm \text{na}$
San San Pond Sak 2 ^b	5.34 ± 0.53	62 ± 25	$0.11 \pm \text{na}$	94.2 ± 0.4	506 ± 250	20.3 ± 12.3	25.2 ± 12	$205 \pm \text{na}$
Damani-Guariviara	5.38 ± 0.55	55 ± 18	$0.11 \pm \text{na}$	92.9 ± 2.1	536 ± 190	15.8 ± 1.5	57.7 ± 13	$50 \pm \text{na}$
Almirante Bay	5.59 ± 0.09	57 ± 10	$0.09 \pm \text{na}$	94.6 ± 0.6	470 ± 40	20.9 ± 2.9	2.1 ± 0.1	$212 \pm \text{na}$

^{a,b} San San Pond Sak sites 1 and 2 correspond to Sites 1 and 2 respectively from Sjögersten *et al.* (2011) 926

Values are mean \pm SE of three peat samples, with the exception of bulk density and P, which were measured from a single sample

Bulk density and total elements are presented in a dry weight basis. na, not available 927

928

929 **Table 3.** Summary of REML outputs: CO₂ and CH₄ fluxes (log₁₀ mg m⁻² h⁻¹).

Table 3. Summary of REML outputs: CO₂ and CH₄ fluxes (log₁₀ mg m⁻² h⁻¹)

	F	df	P
CO₂			
Vegetation community (VC) ^a	0.54	1,4	> 0.05
Water table (WT) ^b	34.71	2,267	< 0.001
Time ^c	10.05	5,266	< 0.001
VC × WT	0.79	2,268	> 0.05
VC × Time	3.45	5,267	< 0.01
WT × Time	6.04	6,267	< 0.001
VC × WT × Time	7.51	2,265	< 0.001
CH₄			
Vegetation community (VC)	0.90	1,4	> 0.05
Water table (WT)	3.26	2,250	< 0.01
Time	15.54	5,250	< 0.001
VC × WT	0.48	2,251	> 0.05
VC × Time	23.44	5,250	< 0.001
WT × Time	3.87	6,251	< 0.001
VC × WT × Time	4.12	2,250	< 0.05

Notes: ^aVegetation community: three *R. taedigera* palm swamps and three *C. panamensis* mixed forests; ^bWater table classification considered: below peat surface, at the surface or above the peat surface; ^cTime corresponds to the six sampling blocks distributed through the year (*i.e.* three during rain and three during dry season)

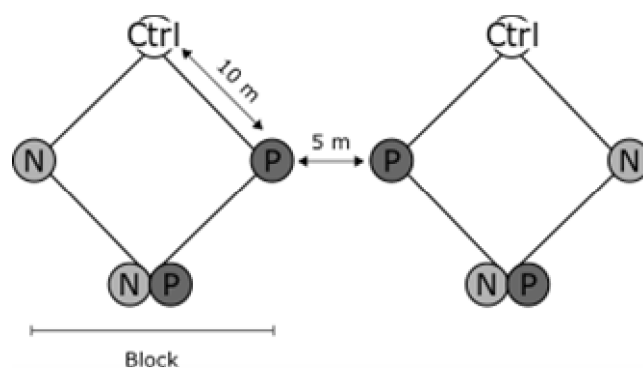
930

931

932 **Figure S1.** Location of palm swamp and mixed forests sites for annual monitoring of CO₂ and CH₄ fluxes from peat surface. The distribution of
933 blocks for the fertilization experiment are presented for the San San Pond Sak 1 and San San Pond Sak 2 sites.

934

935 **Figure S2.** Schematic diagram outlining the experimental set up for the nutrient addition, (Ctrl) control, (N) nitrogen and (P) phosphorous. The
936 diagram is taken from (Hoyos-Santillan et al., 2018). The same set up was used at the palm swamp and the mixed forest sites. Ten blocks were
937 set up at each site with litterbags placed both at the peat surface and at 50 cm depth. Distribution of blocks in San San Pond Sak 1 and San San
938 Pond Sak 2 is presented in Fig. S1.



939

940

941

942

943 **Table S1.** Vegetation survey: Contribution to the total basal area (%) of trees species from individuals with ≥ 10 cm diameter at breast height.

Table S1 Vegetation survey: Contribution to the total basal area (%)*of trees species from individuals with ≥ 10 cm diameter at breast height

Species	Chiriqui	Cricamola	San san pond sak 1 ^a	San san pond sak 2 ^b	Almirante	Damani-Guariviara
<i>Alchornea latifolia</i> Sw.			0.3	0.6	0.1	
<i>Ardisia</i> sp.				1.0	0.4	
<i>Camptosperma panamensis</i> Standl.			0.2	38.7	75.6	77.4
<i>Cassipourea elliptica</i> (Sw.) Poir.				25.0	6.0	
<i>Chrysobalanus icaco</i> L.						
<i>Clusia</i> cf. <i>rosea</i> Jacq.				1.1		0.8
<i>Cyrilla racemiflora</i> L.						
<i>Drypetes standleyi</i> G.L. Webster				1.0	0.5	
<i>Elaeis oleifera</i>	5.51					
<i>Euterpe precatoria</i> Mart.				10.0	1.4	0.6
<i>Fabaceae</i>						5.13
<i>Ficus brevibracteata</i> W.C. Burger			0.3			
<i>Ficus costaricana</i> (Liebm.) Miq.				0.3		
<i>Ficus maxima</i> Mill.			0.2			
<i>Ficus</i> sp.	2.8	3.0		0.3		
<i>Inga</i> sp		0.2				
<i>Myrica mexicana</i> Humb. & Bonpl. ex Willd.						0.6
<i>Manicaria saccifera</i>		22.7				5.6
<i>Maquira guianensis</i>	6.8					
<i>Pterocarpus officinalis</i>	3.71					
<i>Raphia taedigera</i> (Mart.) Mart.	80.5	70.9	98.9		12.5	
<i>Symphonia globulifera</i> L.f.	0.5			21.7	3.2	
<i>Trophis</i>		0.1				

^{a,b} San San Pond Sak sites 1 and 2 data correspond to that from Sites 1 and 2, respectively, from Sjögersten *et al.* (2011)

*Species contributing the most to the proportion of the basal area are presented in bold font.

944

945

946 **Table S2.** Sampling and monitoring dates for greenhouse gas fluxes (mm/dd/yy).

Table S2. Sampling and monitoring dates for greenhouse gas fluxes during wet and dry seasons (mm/dd/y)

Site	Block 1 (wet)	Block 2 (dry)	Block 3 (wet)	Block 4 (wet)	Block 5 (dry)	Block 6 (dry)
Chiriquí Grande	12/16/2010	03/24/2011	05/17/2011	07/06/2011	08/11/2011	09/15/2011
Cricamola River	12/10/2010	03/19/2011	05/28/2011	07/14/2011	08/10/2011	09/14/2011
San San Pond Sak 1 ^a	12/07/2010	03/06/2011	05/16/2011	07/17/2011	08/12/2011	09/16/2011
San San Pond Sak 2 ^b	12/21/2010	01/16/2011	04/27/2011	07/11/2011	08/14/2011	09/11/2011
Damani-Guariviara	12/08/2010	03/17/2011	04/07/2011	07/13/2011	08/09/2011	09/12/2011
Almirante Bay	12/05/2010	03/25/2011	04/06/2011	07/15/2011	08/13/2011	09/13/2011

^{a,b} San San Pond Sak sites 1 and 2 correspond to Sites 1 and 2, respectively from Sjögersten *et al.*, 2010

Gas samples were collected during daylight between 9 am and 4 pm

Wet and dry seasons were defined based on the historic data from the Smithsonian Tropical Research Institute Physical Monitoring Program

947

948

949

950

951

952 **Table S3.** Extractable and microbial dissolved organic carbon (DOC), total dissolved nitrogen (TDN), and readily-exchangeable phosphorus
 953 (REP) at the fertilized plots. Data is presented as mean \pm SE.

Table S3. Extractable and microbial dissolved organic carbon (DOC), total dissolved nitrogen (TDN), and readily-exchangeable phosphorus (REP) at the fertilized plots.

Site	Community	Treatment	DOC ($\mu\text{gC g}^{-1}$)		TDN ($\mu\text{gN g}^{-1}$)		REP ($\mu\text{gP g}^{-1}$)	
			Ext	Mic	Ext	Mic	Ext	Mic
PS1 ^a	Palm swamp	C	240.7 \pm 29.6	1254.7 \pm 266	62.5 \pm 5.9	170.2 \pm 38.0	24.8 \pm 3.0	239.4 \pm 22.3
		N	151.9 \pm 11.4	609.0 \pm 156.7	43.7 \pm 6.9	81.8 \pm 22.6	14.5 \pm 3.3	186.2 \pm 42.8
		P	237.1 \pm 10.4	714.1 \pm 353	67.2 \pm 19.7	102.6 \pm 51.5	243.6 \pm 65.6	149.7 \pm 45.6
		NP	291.5 \pm 86.8	826.2 \pm 303.7	78.3 \pm 22.6	103.9 \pm 32.2	212.1 \pm 44.3	151.1 \pm 70.1
PS2 ^b	Mixed forest	C	176.0 \pm 45.6	331.2 \pm 54.9	46.1 \pm 10.2	40.0 \pm 6.0	7.8 \pm 1.8	146.8 \pm 46.0
		N	159.4 \pm 65.3	296.8 \pm 38.2	886.5 \pm 333.4	144.7 \pm 74.8	5.7 \pm 1.3	79.4 \pm 8.3
		P	234.1 \pm 46.7	371.2 \pm 120.6	50.9 \pm 4.9	53.5 \pm 19.7	73.9 \pm 39	56.7 \pm 14.6
		NP	170.6 \pm 10.9	299.9 \pm 57.9	199.6 \pm 82.3	79.3 \pm 23.2	90.4 \pm 67.4	72.2 \pm 20.9

^{a,b} San San Pond Sak sites 1 and 2 correspond to Sites 1 and 2 respectively from Sjögersten *et al.* (2011)

DOC, TDN, and REP are presented on a dry weight basis

Ext: extractable; Mic: microbial

Data is presented as mean \pm SE of five blocks for each vegetation community

954

955

956

957

958

959 **Table S4.** Summary of linear regression models for CO₂ and CH₄ fluxes (log₁₀ mg m⁻² h⁻¹): physicochemical characteristics of peat and TMAH-
 960 Py-GC/MS analyses.

Table S4. Summary of linear regression models for CO₂ and CH₄ fluxes (log₁₀ mg m⁻² h⁻¹):
 physicochemical characteristics of peat and TMAH-Py-GC/MS analyses

		Intercept	s.e.	t pr.	Slope	s.e.	t pr.	R ²
CO₂								
<u>Physicochemistry and environmental factors</u>								
Rainfall	(mm)	2.469	0.033	< 0.001	-0.0002	0.000	> 0.05	0.00
Water table	(cm)	2.395	0.014	< 0.001	-0.0107	0.001	< 0.001	0.16
Peat depth	(cm)	2.495	0.034	< 0.001	-0.0003	0.000	< 0.05	0.01
Dissolved O ₂ ^a	(ppm)	2.381	0.031	< 0.001	0.0264	0.018	> 0.05	0.00
Temperature ^b	(°C)	1.090	0.544	< 0.05	0.0545	0.021	< 0.05	0.03
C:N	-	2.413	0.078	< 0.001	0.0001	0.001	> 0.05	0.00
<u>Peat composition (µg mgC⁻¹)</u>								
Lignin		2.265	0.047	< 0.001	0.004	0.001	< 0.01	0.00
Fatty Acids								
	Short (< C20)	2.393	0.032	< 0.001	0.0029	0.003	> 0.05	0.00
	Long (> C20)	2.522	0.032	< 0.001	- 0.008	0.002	< 0.001	0.00
Phenolic		2.539	0.038	< 0.001	- 0.109	0.031	< 0.001	0.00
CH₄								
<u>Physicochemistry and environmental factors</u>								
Rainfall	(mm)	0.189	0.114	> 0.05	-0.0013	0.000	< 0.001	0.04
Water table	(cm)	-0.180	0.053	< 0.001	-0.0017	0.005	> 0.05	0.00
Peat depth	(cm)	0.230	0.122	> 0.05	-0.0014	0.000	< 0.001	0.00
Dissolved O ₂	(ppm)	-0.335	0.115	< 0.01	0.0820	0.069	> 0.05	0.00
Temperature	(°C)	-1.630	1.990	> 0.05	0.0603	0.080	> 0.05	0.00

C:N	-	-0.382	0.096	< 0.001	0.0041	0.001	< 0.01	0.00
Peat composition ($\mu\text{g mgC}^{-1}$)		<hr/>						
Lignin		-0.318	0.171	> 0.05	0.004	0.004	> 0.05	0.00
Fatty Acids								
	Short (< C20)	-0.309	0.112	< 0.01	0.020	0.013	> 0.05	0.00
	Long (> C20)	0.534	0.108	< 0.001	-0.051	0.007	< 0.001	0.15
Phenolic		-0.366	0.140	< 0.05	0.186	0.115	> 0.05	0.00

Notes: ^{a,b}Dissolved oxygen, conductivity, and temperature in pore water at the top 50 cm layer of peat.
n.s. = not significant